Synthesis and Pharmacological Evaluation of Novel Pyrazolyl Piperidine Derivatives as Effective Antiplatelet Agents

Jigar Y. Soni,[a] Riyaj S. Tamboli,[b] Rajani Giridhar,[b] Mange Ram Yadav,[b] and Sonal Thakore[a]*

[a]Department of Chemistry, Faculty of Science, The M. S. University of Baroda, Vadodara 390 002, India
[b]Pharmacy Department, Faculty of Technology and Engineering, Kalabhavan, The M. S. University of Baroda, Vadodara 390 001, India
*E-mail: chemistry2797@yahoo.com

Additional Supporting Information may be found in the online version of this article.
Received January 30, 2016
DOI 10.1002/jhet.2703
Published online 00 Month 2016 in Wiley Online Library (wileyonlinelibrary.com).

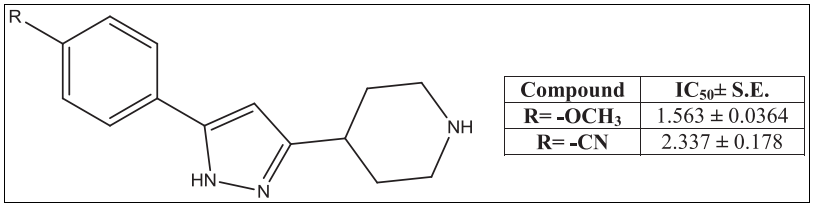

Compound	IC_{50}± S.E.
R= -OCH_3	1.563 ± 0.0364
R= -CN	2.337 ± 0.178

The synthesis and antiplatelet activity of substituted pyrazolyl piperidine derivatives (**3a–n**) are described. These compounds were synthesized by an improved ring opening reaction of 2-arylidene quinuclidinone using hydrazine hydrate under mild conditions. They were characterized and screened for their *in vitro* antiplatelet profile in human platelet aggregation using adenosine diphosphate as agonist. Investigation of structure activity relation revealed interesting results. Among these synthesized derivatives (**3a–n**), compounds **3a**, **3c**, **3j**, and **3l** exhibited excellent activity, while **3c** was the most potent one. Based on IC_{50} values, it was observed that most of the compounds possessed antiplatelet aggregation activity superior to the reference drug Aspirin.

J. Heterocyclic Chem., **00,** 00 (2016).

INTRODUCTION

Atherothrombotic coronary artery disease gives rise to a number of cardiocirculatory disorders such as myocardial infarction, unstable angina, or acute stroke associated with deep vein thrombosis [1]. Hence, it is a growing public health problem and one of the most common causes of death worldwide. The abnormal formation of intravascular occlusions is the main cause of these diseases. Hence, the prevention of thrombogenesis has become a vital target in the prophylaxis and therapy of cardiocirculatory disorders with thromboembolic complications [2]. According to World Health Organization, stroke is responsible for millions of deaths and stroke-related disability [3]. Thrombosis may occur when the hemostatic stimulus becomes unregulated. Important predisposing conditions to thrombosis are disturbed blood flow, hyper coagulation, and altered vessel wall [4]. Arterial thrombi are predominantly composed of platelets, a small amount of fibrin, and a few red blood cells. Because of this, the antiplatelet agents are successfully used in the treatment and prevention of arterial thrombosis. The relevance of antiplatelet drugs has been firmly established by clinical trials and experienced with drugs, such as aspirin, dipyridamole, and thienopyridines [5–7]. These drugs are the only oral antiplatelet agents currently approved by the Food and Drug Administration for use in patients. Recently, antiplatelet combination therapy using agents with different mechanisms of action seems to be an attractive preventive approach, because different signaling pathways contribute to platelet activation [8]. Three classes of antiplatelet agents are currently approved for clinical use and get specific recommendations from clinical guidelines for practical management of patients with acute coronary syndrome or those undergoing percutaneous coronary intervention (Fig. 1): (i) cyclooxygenase-1 inhibitors (aspirin); (ii) glycoprotein IIb/IIIa inhibitors (eptifibatide, abciximab, and tirofiban); and (iii) adenosine diphosphate (ADP) P2Y12 receptor antagonists (ticlopidine, clopidogrel, ticagrelor, and prasugrel) [9].

Clinical studies have demonstrated their efficacy in the minimizing ischemic recurrences and prevention of thromboembolic disease, but these are accompanied by side effects such as gastrointestinal toxicity because of aspirin including nausea, vomiting, dyspepsia, heartburn, gastrointestinal ulceration, and so on. In recent years, the issue of resistance to antiplatelet agents, in particular, aspirin and thienopyridines, has been highlighted in the medical literature [10–13].

In short, the treatment of acute coronary syndrome and its complications, especially the clinical management of aspirin and clopidogrel resistance, still demand much attention [14]. Novel effective antiplatelet agents with fast initiation of action and low risks of bleeding are still needed. In search of newer more potent antiplatelet agents with high activity and minimum side effects, some novel substituted

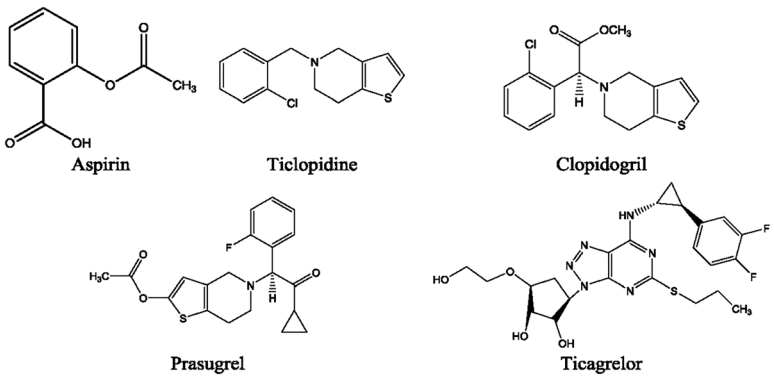

Figure 1. Structures of currently available antiplatelet drugs.

pyrazolyl piperidine derivatives were screened with antiplatelet activity [14].

Quinuclidinone hydrochloride is an important building block of many Food and Drug Administration-approved drugs like Solifenacin, Azasetron, Quinupramine, and so on and possesses a wide spectrum of biological activity. Its analogs are known for $\alpha 7$ and $\alpha 4\beta 2$ nicotinic receptors inhibitory activity [15], Alzheimer's disease [16], and antihistamine-bronchodilating agents [17]. Therefore, we focused our attention on the synthesis of some pyrazolyl piperidine derivatives from quinuclidinone hydrochloride with a view to evaluate their antiplatelet activity

RESULT AND DISCUSSION

Synthesis of pyrazolyl piperidine derivative. In the first step, the starting material 3-quinuclidinone hydrochloride **1** was prepared as per the procedure described in our previous report [18,19]. It was converted into compounds **2a–n** with various substituted aromatic aldehydes in the presence of sodium hydroxide, using absolute ethanol as solvent (Scheme 1). Finally, the new pyrazolyl piperidine compounds (**3a–n**) were prepared by improved method in good yields only by refluxing the product of the first step with excess of hydrazine hydrate [20].

Biological assay and structure activity relationship evaluations [14]. To confirm the potentiality of the pyrazolyl piperidine moiety for designing new antiplatelet agents, the pyrazolyl piperidine derivatives (**3a–n**) were screened as our previous protocol described in Supporting Information. Initially, target compounds were screened at 100 μM for inhibitory effects on human platelets aggregation using ADP as agonist. Interestingly, almost all compounds presented a significant inhibitory profile at this concentration. All the compounds were screened thrice at 5, 10, and 15 μM concentrations, and experimental half-maximal inhibitory concentration (IC_{50}) was calculated (Table 1).

Scheme 1. Synthesis of pyrazolyl piperidine compounds (**3a–n**) by using 3-quinuclidinone hydrochloride.

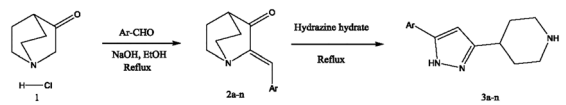

For the synthesized compounds (**3a–n**), the IC_{50} of all derivatives was comparable with aspirin, the most used antiplatelet drug currently in the market (Fig. 2).

The determination of IC_{50} on ADP-induced platelet aggregation assays showed two different levels of antiplatelet activity that included values lower (1.53–14.78 μM) as well as similar (16.5–24.07 μM) to aspirin (16.5 ± 0.2 μM). The correlation of structure with activity for our compounds revealed interesting results. The derivatives with methoxy group (**3a–c**) were most potent, while those with nitro group showed least activity. Except *p*-nitro compound (**3d**), all other nitro-derivatives did not show any activity. Methoxy group at *p*-position (**3a**) increases the activity, while that at *o*-position (**3b**) decreases the activity. But when an additional methoxy group was introduced as in compound (**3c**), the activity was improved. The substrate with chloro group at paraposition (**3e**) showed least activity that further improved when both the *ortho* position were substituted by chloro group (**3f**). Substitution by various halogens affected the activity significantly. Among halogens, fluoro (**3h**) gives better activity than chloro (**3e**). An additional methoxy group (**3i**) does have much impact on the activity of fluoro compound. The cyano group (**3j**) and methyl group at *p*-position (**3a**) did not have any enhancement in the activity significantly. Instead of chlorophenyl (**3e**), chloro pyridyl derivative (**3l**) showed much higher activity almost comparable with methoxy phenyl derivative (**3a**). The best profile (1.53–14.78 μM) was observed for compounds **3a**, **3c**, **3l**, and **3j**. On the basis of structure activity relationship, the order of activity of different compounds can be summarized as **3c > 3a > 3l > 3j > 3k > 3f > 3i > 3h > 3b > 3e > 3g > 3d**.

Table 1

Structure and IC_{50} values of target compounds (**3a–n**)

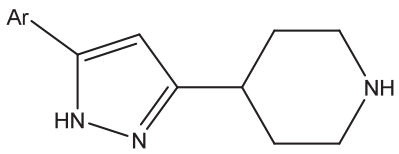

Compound	Ar	IC_{50} (μM) ± SE	Compound	Ar	IC_{50} (μM) ± SE
3a	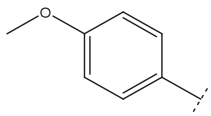	1.563 ± 0.0364	**3h**	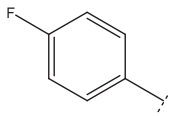	4.988 ± 0.076
3b	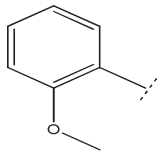	8.495 ± 0.053	**3i**	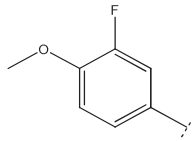	4.771 ± 0.048
3c	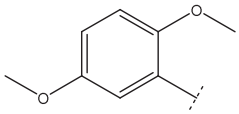	1.435 ± 0.053	**3j**	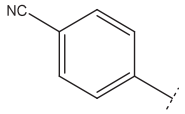	2.337 ± 0.178
3d	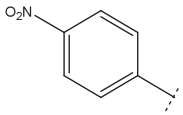	24.07 ± 0.119	**3k**	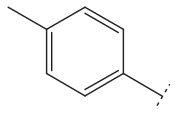	3.717 ± 0.055
3e	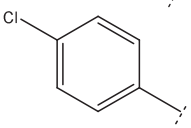	14.78 ± 0.145	**3l**	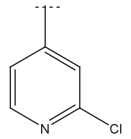	1.884 ± 0.070
3f	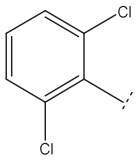	3.786 ± 0.06	**3m**	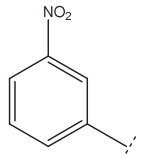	–
3g	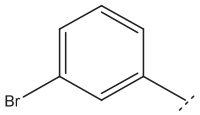	16.46 ± 0.143	**3n**	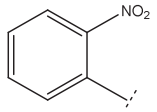	–

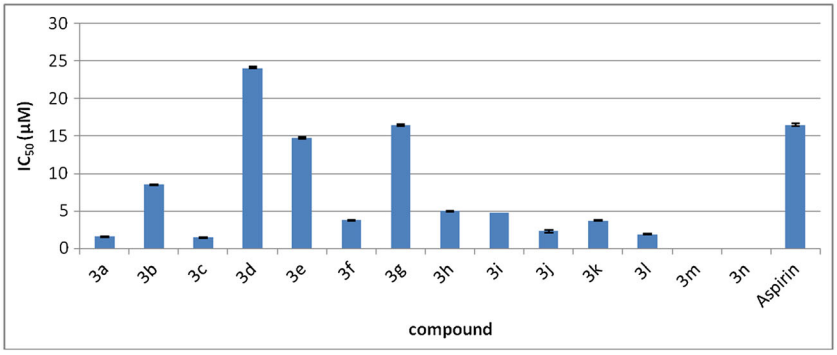

Figure 2. The IC_{50} values of target compounds (**3a–n**). [Color figure can be viewed in the online issue, which is available at wileyonlinelibrary.com.]

CONCLUSION

In summary, based on our biological results, we identified some of the synthesized pyrazolo-piperidine derivatives as potential lead compounds and significant inhibitors ($IC_{50} > 20\,\mu M$) **3a**, **3c**, **3l**, and **3j** for further *in vitro* and *in vivo* investigation. Interestingly, the antiplatelet profile of these compounds offered promising results when compared with standard aspirin.

EXPERIMENTAL

Material and methods

Chemistry. Commercial grade solvents and reagents were purchased from Sigma-Aldrich or Alfa Aesar or Spectrochem Mumbai and used without further purification. Quinuclidinone hydrochloride was prepared as per the procedure described in our previous report [18,19]. Melting points were measured using a (Buchi B-545) melting point apparatus and are uncorrected. Infrared spectra were recorded on Perkin-Elmer RX 1 and Perkin-Elmer 580B spectrometer (Perkin-Elmer, Waltham, MA). Elemental analyses were recorded on Thermosinnigan flash 11-12 series EA. ^{1}H and ^{13}C NMR spectra were recorded on advance Bruker (400 MHz) spectrometer in suitable deuterated solvents. ^{1}HNMR data were recorded as follows: chemical shift measured in parts per million (ppm) downfield from trimethylsilyl (d), multiplicity, observed coupling constant (*J*) in hertz (Hz), and proton count. Multiplicities are reported as singlet (s), broad singlet (br s), doublet (d), triplet (t), quartet (q), and multiplet (m). ^{13}C NMR chemical shifts are reported in ppm downfield from trimethylsilyl, and identifiable carbons are given. Solvents and reagents were purified by literature methods. Mass spectra were determined by electrospray ionization (ESI)/mass spectrometry (MS), using a Shimadzu LCMS 2020. The reaction progress was monitored by thin-layer chromatography (TLC) in ultraviolet light as well as in iodine vapor. Platelet aggregation study was performed by using Chrono-Log model 592VS dual-channel whole blood aggregometer from Chrono-Log Corporation (Havertown, PA, USA).

Biology. Platelet aggregation study was performed as per our previous protocol [14] by using Chrono-Log model 592VS dual-channel whole blood aggregometer from Chrono-Log Corporation. Electrical impedance method was used with 450 µL of whole human blood withdrawn from healthy human volunteers. It was diluted with 450 µL phosphate buffered saline and then incubated at 37°C. Blood sample was equilibrated for 2 min for getting stable baseline. A total of 10 µL of test sample was added followed by addition of 10 µL of ADP while stirring at 1000 rpm. The maximum impedance value was determined, and results were analyzed using Aggrolink version 4.75 software up to 6 min. The IC_{50} values were calculated by using three individual experiments at three different concentrations (*viz.* 5, 10, and 15 µM).

General procedure for preparation of compounds 2a–n. The reaction of equimolar proportion of compound **1** and aromatic-substituted aldehyde in presence of equimolar proportion of sodium hydroxide in absolute ethanol refluxed. The progress of the reaction was monitored by TLC. After completion, the solvent was evaporated in underreduced pressure. The residue was dissolved in ethyl acetate (50 mL) and washed with water. Organic layer was dried with sodium sulfate and solvent evaporated in vacuum. The yellow solid obtained was recrystallized from IPA/H_2O (1:1) (compounds **2d** and **2i–2k**) or absolute methanol (compound **2e**).

General procedure for the preparation of compounds 3a–n. The product of step one (**2a–n**) was taken in excess base hydrazine hydrate and refluxed to give title compounds (**3a–n**). The progress of the reaction was monitored by TLC. After completion, the reaction mixture was allowed to cool to room temperature. A crystalline solid precipitated that was filtered and washed with water. Drying under *vacuum* afforded pure desired compounds **3a–n**.

(Z)-2-(4-methoxybenzylidene)quinuclidin-3-one (2a). Yellow solid, mp 105–108°C (rep 106–108°C) [21]; yield 78%; reaction time 2 h and 30 min. ^{1}H NMR (400 MHz, $CDCl_3$): δ 1.99–2.04 (4H, m, CH_2); 2.61–2.63 (1H, m, CH); 2.94–3.02 (2H, m, CH_2); 3.12–3.19 (2H, m, CH_2); 3.84 (3H, s, OCH_3); 6.90–6.91 (2H, d, $J = 8.8$ Hz, ArH); 6.99 (1H, s, vinylic proton); 8.03–8.05 (2H, d, $J = 9.2$ Hz, ArH). ^{13}C NMR (100 MHz, $CDCl_3$): δ 26.0, 40.3, 47.5, 55.3, 55.4, 93.3, 113.9, 114.2, 114.5, 125.1, 126.7, 129.1, 130.1, 134.0, 134.2, 142.7, 150.1, 160.7, 206.5. IR (KBr, cm^{-1}): 3061, 3024, 2950, 2835, 1699, 1255. ESI/MS 244.2 $[M+1]^+$ calculated for $C_{15}H_{17}NO_2$. *Anal.* Calcd. for $C_{15}H_{17}NO_2$: C, 74.05; H, 7.04; N, 5.76; Found: C, 74.29; H, 6.83; N, 5.61.

(Z)-2-(2-methoxybenzylidene)quinuclidin-3-one (2b). Yellow solid, mp 112–114°C; yield 82%; reaction time 4 h. ^{1}H NMR (400 MHz, $CDCl_3$): δ 2.02–2.07 (4H, m, CH_2); 2.64–2.66 (1H, m, CH); 2.98–3.05 (2H, m, CH_2); 3.15–3.22 (2H, m, CH_2); 3.84 (3H, s, OCH_3); 6.90–6.93 (1H, dd, $J = 4.0$, 0.8 Hz, ArH) 7.00 (1H, s, vinylic proton); 7.28–7.32 (1H, t, $J = 8.0$, 7.6 Hz, ArH); 7.53–7.55 (1H, d, $J = 7.2$ Hz, ArH); 7.81 (1H, s, ArH). ^{13}C NMR (100 MHz, $CDCl_3$): δ 25.8, 40.3, 47.4, 55.2, 115.4, 117.0, 124.9, 125.0, 129.3, 135.2, 145.0, 159.4, 159.9, 206.5. IR (KBr, cm^{-1}): 3069, 3031, 3011, 2955, 2837, 1706, 1040. ESI/MS 244.2 $[M+1]^+$ calculated for $C_{15}H_{17}NO_2$. *Anal.* Calcd. for $C_{15}H_{17}NO_2$: C, 74.05; H, 7.04; N, 5.76; Found: C, 73.89; H, 7.28; N, 5.89.

(Z)-2-(2,5-dimethoxybenzylidene)quinuclidin-3-one (2c). Yellow solid, mp 128–130°C; yield 73%; reaction time 2 h and 30 min. ^{1}H NMR (400 MHz, $CDCl_3$): δ 1.93–1.96 (4H, m, CH_2); 2.54–2.57 (1H, m, CH); 2.88–2.95 (2H, m, CH_2); 3.04–3.11 (2H, m, CH_2); 3.71 (3H, s, OCH_3); 3.74 (3H, s, OCH_3); 6.72–6.74 (1H, d, J = 8.8 Hz, ArH); 6.79–6.82 (1H, d, J = 3.2 Hz, ArH); 7.19 (1H, s, vinylic proton); 7.45 (1H, s, ArH) 8.23–8.24 (1H, d, J = 2.8 Hz, ArH). ^{13}C NMR (100 MHz, $CDCl_3$): δ 25.9, 40.3, 47.5, 55.7, 56.1, 111.4, 116.1, 117.8, 118.7, 123.3, 144.5, 153.0, 153.7, 206.3. IR (KBr, cm^{-1}): 3308, 3080, 3015, 2945, 2835, 1698, 979. ESI/MS 274.3 $[M+1]^+$ calculated for $C_{16}H_{19}NO_3$. *Anal.* Calcd. for $C_{16}H_{19}NO_3$: C, 70.31; H, 7.01; N, 5.12; Found: C, 70.12; H, 7.23; N, 4.99.

(Z)-2-(4-nitrobenzylidene)quinuclidin-3-one (2d). Yellow solid, mp 127–129°C (rep 126–128°C) [22]; yield 48%; reaction time 6 h. ^{1}H NMR (400 MHz, $CDCl_3$): δ 1.98–2.06 (4H, m, CH_2); 2.60–2.63 (1H, m, CH); 2.88–2.96 (2H, m, CH_2); 3.10–3.17 (2H, m, CH_2); 6.95 (1H, s, vinylic proton); 8.10–8.15 (4H, s, ArH). ^{13}C NMR (100 MHz, $CDCl_3$): δ 32.8, 34.2, 46.4, 100.5, 124.1, 126.0, 139.6, 147.1, 149.1, 150.7. IR (KBr, cm^{-1}): 3310, 3062, 1708, 1526, 1333, 1098, 994, 854, 679. ESI/MS 259.3 $[M+1]^+$ calculated for $C_{14}H_{14}N_2O_3$. *Anal.* Calcd. for $C_{14}H_{14}N_2O_3$: C, 65.11; H, 5.46; N, 10.85; Found: C, 65.35; H, 5.29; N, 10.68.

(Z)-2-(4-chlorobenzylidene)quinuclidin-3-one (2e). Yellow solid, mp 114–116°C (rep 112.5–114.5°C) [23]; yield 83%; reaction time 2 h. ^{1}H NMR (400 MHz, $CDCl_3$): δ 2.06–2.08 (4H, m, CH_2); 2.64–2.67 (1H, m, CH); 2.94–3.03 (2H, m, CH_2); 3.13–3.21 (2H, m, CH_2); 6.97 (1H, s, vinylic proton); 7.33–7.36 (2H, m, ArH); 7.98–8.02 (2H, m, ArH).^{13}C NMR (100 MHz, $CDCl_3$): δ 25.8, 40.2, 47.4, 123.7, 128.7, 133.3, 135.4, 145.0, 206.2. IR (KBr, cm^{-1}): 1709, 1308, 1166, 1096. ESI/MS 247.9 $[M]^+$, 249.2 $[M+2]^+$ calculated for $C_{14}H_{14}NOCl$. *Anal.* Calcd. for $C_{14}H_{14}NOCl$: C, 67.88; H, 5.70; N, 5.65; Found: C, 68.13; H, 5.47; N, 5.43.

(Z)-2-(2,6-dichlorobenzylidene)quinuclidin-3-one (2f). Yellow solid, mp 121–123°C (rep 118–120°C) [24]; yield 81%; reaction time 4 h and 30 min. ^{1}H NMR (400 MHz, $CDCl_3$): δ 1.94–2.11 (4H, m, CH_2); 2.67–2.69 (1H, m, CH); 3.02–3.08 (4H, m, CH_2); 7.03 (1H, s, vinylic proton); 7.17–7.22 (1H, dd, J = 8.4, 8.0 Hz, ArH); 7.31–7.35 (2H, d, J = 8.0 Hz, ArH). ^{13}C NMR (100 MHz, $CDCl_3$): δ 25.6, 40.5, 47.3, 122.1, 127.7, 127.8, 129.4, 132.9, 134.1, 147.9 204.8. IR (KBr, cm^{-1}): 3055, 3023, 1713, 1103, 979, 851. ESI/MS 282.2 $[M]^+$, 284.2 $[M+2]^+$ calculated for $C_{14}H_{13}NOCl_2$. *Anal.* Calcd. for $C_{14}H_{13}NOCl_2$: C, 59.59; H, 4.64; N, 4.96; Found: C, 59.73; H, 4.52; N, 4.82.

(Z)-2-(3-bromobenzylidene)quinuclidin-3-one (2g). Yellow solid, mp 138–140°C; yield 79%; reaction time 3 h. ^{1}H NMR (400 MHz, $CDCl_3$): δ 2.02–2.07 (4H, m, CH_2); 2.65–2.67 (1H, m, CH); 2.98–3.03 (2H, m, CH_2); 3.15–3.23 (2H, m, CH_2); 6.98 (1H, s, vinylic proton); 7.04–7.05 (1H, t, J = 2.8, 2, 0.8 Hz, ArH); 7.30–7.36 (1H, m, ArH); 7.59–7.61 (1H, d, J = 8 Hz, ArH); 8.06–8.10 (1H, t, J = 8.4 Hz, ArH). ^{13}C NMR (100 MHz, $CDCl_3$): δ 25.7, 40.1, 47.4, 116.4, 116.7, 118.1, 118.3, 112.7, 123.7, 128.1, 128.2, 129.7, 129.8, 135.9, 136.0, 145.6, 161.4, 163.8, 206.2. IR (KBr, cm^{-1}): 3083, 3043, 2964, 2938, 1701, 978. ESI/MS 292 $[M]^+$, 294 $[M+2]^+$ calculated for $C_{14}H_{14}NBrO$. *Anal.* Calcd. for $C_{14}H_{14}NBrO$: C, 57.55; H, 4.83; N, 4.79; Found: C, 57.32; H, 4.95; N, 4.64.

(Z)-2-(4-fluorobenzylidene)quinuclidin-3-one (2h). Yellow solid, mp 117–118°C (rep 118–120°C) [21]; yield 81%; reaction time 30 min. ^{1}H NMR (400 MHz, $CDCl_3$): δ 2.02–2.06 (4H, m, CH_2); 2.64–2.65 (1H, m, CH); 2.95–3.02 (2H, m, CH_2); 3.13–3.20 (2H, m, CH_2); 6.98 (1H, s, vinylic proton); 7.04–7.08 (2H, m, ArH); 8.05–8.09 (2H, q, ArH). ^{13}C NMR (100 MHz, $CDCl_3$): δ 25.8, 40.2, 47.8, 115.4, 115.6, 123.8, 130.2, 130.2, 134.2, 134.2, 144.1, 144.2, 162.0, 164.5, 206.3. IR (KBr, cm^{-1}): 3098, 3060, 1698, 1257, 1221, 1035, 995. ESI/MS 232.2 $[M+1]^+$ calculated for $C_{14}H_{14}NOF$. *Anal.* Calcd. for $C_{14}H_{14}NOF$: C, 72.71; H, 6.10; N, 6.06; Found: C, 72.94; H, 5.93; N, 5.93.

(Z)-2-(3-fluoro-4-methoxybenzylidene)quinuclidin-3-one (2i). Yellow solid, mp 108–110°C; yield 64%; reaction time 2 h. ^{1}H NMR (400 MHz, $CDCl_3$): δ 2.01–2.05 (4H, m, CH_2); 2.62–2.64 (1H, m, CH); 2.95–3.00 (2H, m, CH_2); 3.01–3.19 (2H, m, CH_2); 3.92 (3H, S, OCH_3) 6.91–6.95 (2H, m, ArH + vinylic proton); 7.50–7.52 (1H, d, J = 8.0 Hz, ArH); 8.25–8.29 (1H, dd, J = 1.6, 2 Hz, ArH). ^{13}C NMR (100 MHz, $CDCl_3$): δ 25.9, 40.2, 47.4, 56.1, 112.5, 118.8, 119, 123.8, 127.28, 127.36, 129.4, 143.8, 148.8, 148.9, 150.6, 153.11. IR (KBr, cm^{-1}): 3093, 3075, 1700, 1304, 1169, 686, 518. ESI/MS 262.1 $[M+1]^+$ calculated for $C_{15}H_{16}NO_2F$. *Anal.* Calcd. for $C_{15}H_{16}NO_2F$: C, 68.95; H, 6.17; N, 5.36; Found: C, 68.81; H, 6.39; N, 5.59.

(Z)-4-((3-oxoquinuclidin-2-ylidene)methyl)benzonitrile (2j). Yellow solid, mp 157–159°C [25]; yield 79%; reaction time 4 h. ^{1}H NMR (400 MHz, $CDCl_3$): δ 2.05–2.07 (4H, m, CH_2); 2.66–2.67 (1H, m, CH); 2.96–3.02 (2H, m, CH_2); 3.15–3.23 (2H, m, CH_2); 6.97 (1H, s, vinylic proton); 7.63–7.65 (2H, d, J = 8.4 Hz, ArH); 8.12–8.14 (2H, d, J = 8.4 Hz, ArH). ^{13}C NMR (100 MHz, $CDCl_3$): δ 25.6, 40.0, 47.3, 112.3, 118.8, 122.6, 127.4, 132.0, 132.2, 138.3, 147.1 205.8. IR (KBr, cm^{-1}): 3083, 3043, 2964, 2938, 2265, 2229, 1701. ESI/MS 239 $[M+1]^+$ calculated for $C_{15}H_{14}N_2O$. *Anal.* Calcd. for $C_{15}H_{14}N_2O$: C, 75.61; H, 5.92; N, 11.76; Found: C, 75.79; H, 5.77; N, 11.58.

(Z)-2-(4-methylbenzylidene)quinuclidin-3-one (2k). Yellow solid, mp 115–117°C (rep 118–120°C) [26]; yield 82%; reaction time 3 h and 30 min. ^{1}H NMR (400 MHz, $CDCl_3$): δ 2.03–2.09 (4H, m, CH_2); 2.39 (3H, S, CH_3); 2.67–2.68 (1H, m, CH); 2.96–3.06 (2H, m, CH_2); 3.16–3.24 (2H, m, CH2); 7.04 (1H, s, vinylic proton); 7.19–7.21 (2H, dd, J = 8.0 Hz, ArH); 7.93–7.95 (2H, d, J = 8.4 Hz, ArH). ^{13}C

NMR (100 MHz, $CDCl_3$): δ 21.6, 25.8, 40.2, 47.6, 124.7, 125.4, 129.2, 132.1, 140.1 206.4. IR (KBr, cm^{-1}): 3083, 3043, 2964, 2938, 1701. ESI/MS 228.2 $[M+1]^+$ calculated for $C_{15}H_{17}NO$. *Anal.* Calcd. for $C_{15}H_{17}NO$: C, 79.26; H, 7.54; N, 6.16; Found: C, 79.01; H, 7.69; N, 6.30.

(Z)-2-((3-chloropyridine-4yl)methylene)quinuclidin-3-one (2l). Brown solid, mp 120–122°C; yield 46%; reaction time 2 h. ^1H NMR (400 MHz, $CDCl_3$): δ 2.02–2.09 (4H, m, CH_2); 2.67–2.68 (1H, m, CH); 2.96–3.04 (2H, m, CH_2); 3.16–3.24 (2H, m, CH_2); 6.92 (1H, s, vinylic proton); 7.84–7.85 (1H, dd, J = 7.2, 1.6 Hz, ArH); 8.62–8.63 (2H, d, J = 4.4, 1.6 Hz, ArH). ^{13}C NMR (100 MHz, $CDCl_3$): δ 25.5, 40.0, 47.3, 122.1, 125.4, 140.9, 148.4, 150.1, 205.7. IR (KBr, cm^{-1}): 3080, 3010, 1709, 1600, 1430. ESI/MS 249 $[M]^+$, 251$[M+2]^+$ calculated for $C_{13}H_{13}N_2OCl$. *Anal.* Calcd. for $C_{13}H_{13}N_2OCl$: C, 62.78; H, 5.27; N, 11.26; Found: C, 62.99; H, 5.00; N, 11.41.

(Z)-2-(3-nitrobenzylidene)quinuclidin-3-one (2m). Yellow solid, mp 123–125°C; yield 44%; reaction time 6 h and 30 min. ^1H NMR (400 MHz, $CDCl_3$): δ 1.98–2.06 (4H, m, CH_2); 2.60–2.63 (1H, m, CH); 2.89–2.96 (2H, m, CH_2); 3.10–3.17 (2H, m, CH_2); 6.95 (1H, s, vinylic proton); 8.10–8.15 (4H, s, ArH). ^{13}C NMR (100 MHz, $CDCl_3$): δ 25.5, 40.1, 47.3, 122.1, 123.5, 132.6, 140.3, 147.5, 205.8. IR (KBr, cm^{-1}): 3062, 1708, 1526, 1338, 1098, 994, 854, 679. ESI/MS 259.3 $[M+1]^+$ 259 calculated for $C_{14}H_{14}N_2O_3$. *Anal.* Calcd. for $C_{14}H_{14}N_2O_3$: C, 65.11; H, 5.46; N, 10.85; Found: C, 64.89; H, 5.59; N, 10.99.

(Z)-2-(2-nitrobenzylidene)quinuclidin-3-one (2n). Yellow solid, mp 120–122°C; yield 38%; reaction time 3 h. ^1H NMR (400 MHz, $CDCl_3$): δ 2.02–2.07 (4H, m, CH_2); 2.66–2.69 (1H, m, CH); 2.90–2.98 (2H, m, CH_2); 3.06–3.13 (2H, m, CH_2); 7.38 (1H, s, vinylic proton); 7.46–7.50 (1H, m, ArH); 7.60–7.65 (1H, m, ArH); 7.89–7.91 (1H, dd, J = 8.0, 1.2 Hz, ArH); 7.98–8.00 (1H, dd, J = 8.0, 1.2 Hz, ArH). ^{13}C NMR (100 MHz, $CDCl_3$): δ 25.4, 40.1, 47.5, 121.3, 124.4, 128.9, 129.3, 132.5, 132.7, 146.2, 149.2, 205.1. IR (KBr, cm^{-1}): 3318, 3042, 2940, 2921, 2862, 1556, 1702, 1319, 893, 705. ESI/MS 259.3 $[M+1]^+$ calculated for $C_{14}H_{14}N_2O_3$. *Anal.* Calcd. for $C_{14}H_{14}N_2O_3$: C, 65.11; H, 5.46; N, 10.85; Found: C, 65.36; H, 5.19; N, 10.71.

4-(5-(4-Methoxyphenyl)-1H-pyrazol-3-yl)piperidine (3a). White solid, mp 180–182°C (rep. 181–182°C) [27]; yield 74%; reaction time 20 min. ^1H NMR (400 MHz, $CDCl_3$): δ 1.66–1.76 (2H, m, CH_2); 1.72–1.76 (2H, m, CH_2); 2.73–2.79 (2H, m, CH); 2.81–2.86 (1H,m, CH) 3.19–3.22 (2H, m, CH_2); 3.85 (3H, s, OCH_3) 6.32 (1H, s, pyrazol proton); 6.94–6.96 (2H, d, J = 8.4 Hz) 7.64–7.66 (2H, d, ArH, J = 8.8 Hz). ^{13}C NMR (100 MHz, $CDCl_3$): δ 33.0, 46.5, 55.31, 99.1, 114.1, 125.0, 126.8, 159.4. IR (KBr, cm^{-1}): 3071, 3005, 1304, 1251, 984. ESI/MS 258.2 $[M+1]^+$ calculated for $C_{15}H_{19}N_3O$. *Anal.* Calcd. for $C_{15}H_{19}N_3O$: C, 70.01; H, 7.44; N, 16.33; Found: C, 69.80; H, 7.69; N, 16.56.

***24-(5-(2-Methoxyphenyl)-1H-*pyrazol-3-yl)piperidine (3b).** White solid, mp 160–162°C; yield 64%; reaction time 30 min. ^1H NMR (400 MHz, $CDCl_3$): δ 1.76–1.77 (2H, m, CH_2); 1.99–2.02 (2H, m, CH_2); 2.74–2.89 (3H, m, CH, CH_2); 3.21–3.24 (2H, d, CH_2); 3.86 (3H, s, OCH_3) 6.38 (1H, s, pyrazol proton); 6.87–6.90 (1H, dd, ArH, J = 4.8,2.4 Hz,); 7.29–7.33 (3H, m, ArH). ^{13}C NMR (100 MHz, $CDCl_3$): δ 32.9, 34.6, 44.4, 55.3, 99.8, 110.8, 113.7, 118.1, 129.8, 159.9. IR (KBr, cm^{-1}): 3059, 3003, 2942, 2828, 1036. ESI/MS 258.2 $[M+1]^+$ calculated for $C_{15}H_{19}N_3O$. *Anal.* Calcd. for $C_{15}H_{19}N_3O$: C, 70.01; H, 7.44; N, 16.33; Found: C, 70.34; H, 7.28; N, 16.19.

***4-(5-(2, 5-Dimethoxyphenyl)-1H-*pyrazol-3-yl)piperidine (3c).** White solid, mp 158–160°C; yield 89%; reaction time 1 h and 45 min. ^1H NMR (400 MHz, $CDCl_3$): δ 1.66–1.76 (2H, m, CH_2); 2.02–2.05 (2H, m, CH_2); 2.76–2.82 (2H, m, CH_2); 2.84–2.90 (1H, m, CH_2); 3.19–3.22 (2H, d, CH_2); 3.84 (3H, s, OCH_3), 3.94 (3H, s, OCH_3); 6.47 (1H, s, pyrazol proton); 6.83–6.86 (1H, dd, J = 8.8, 2.8 Hz); 6.93–6.96 (1H, d, J = 8.8 Hz); 7.20–7.28 (1H, d, ArH, J = 2.8 Hz). ^{13}C NMR (100 MHz, $CDCl_3$): δ 33.3, 35.9, 46.7, 55.8, 56.3, 100.0, 112.7, 113.2, 113.9, 141.3, 150.3, 153.9, 156.7. IR (KBr, cm^{-1}): 3298, 2942, 2833, 1048, 1000. ESI/MS 288.3 $[M+1]^+$ calculated for $C_{16}H_{21}N_3O_2$. *Anal.* Calcd. for $C_{16}H_{21}N_3O_2$: C, 66.88; H, 7.37; N, 14.62; Found: C, 67.03; H, 7.26; N, 14.74.

***4-(5-(4-Nitrophenyl)-1H-*pyrazol-3-yl)piperidine (3d).** Yellow solid, mp 168–170°C; yield 78%; reaction time 1 h and 10 min. ^1H NMR (400 MHz, $CDCl_3$): δ 1.73–1.83 (2H, m, CH_2); 2.00–2.04 (2H, m, CH_2); 2.76–2.79 (2H, m, CH_2); 2.82–2.89 (1H, m, CH); 3.23–3.26 (2H, m, CH_2); 6.50 (1H, s, pyrazol proton); 7.94–7.96 (2H, d, ArH, J = 8.8 Hz,); 8.27–8.29 (2H, d, ArH, J = 8.8 Hz). ^{13}C NMR (100 MHz, DMSO + $CDCl_3$): δ 37.7, 38.9, 34.2, 51.2, 104.4, 128.6, 130.4, 139.0, 144.4, 151.2. IR (KBr, cm^{-1}): 3317, 1602, 1508, 1336, 853. ESI/MS 273.0 $[M+1]^+$ calculated for $C_{14}H_{16}N_4O_2$. *Anal.* Calcd. for $C_{14}H_{16}N_4O_2$: C, 61.75; H, 5.92; N, 20.58; Found: C, 62.01; H, 5.74; N, 20.41.

***4-(5-(4-Chlorophenyl)-1H-*pyrazol-3-yl)piperidine (3e).** White solid, mp 185–187°C (rep 186–187°C) [27]; yield 83%; reaction time 40 min. ^1H NMR (400 MHz, $CDCl_3$): δ 1.67–1.77 (2H, m, CH_2); 1.94–1.97 (2H, m, CH_2); 2.67–2.73 (2H, m, CH); 2.76–2.84 (1H, m, CH) 3.15–3.18 (2H, m, CH_2); 6.34 (1H, s, pyrazol proton); 7.34–7.36 (2H, m, ArH, J = 8.4 Hz); 7.66–7.68 (2H, d, J = 8.6 Hz, ArH). ^{13}C NMR (100 MHz, $CDCl_3$): δ 33.0, 34.5, 46.5, 99.6, 126.9, 128.9, 131.4, 133.5, 149.2, 151.6. IR (KBr, cm^{-1}): 3068, 1364, 1265, 1004, 907. ESI/MS 262.2 $[M]^+$, 264.2 $[M+2]^+$ calculated for $C_{14}H_{16}N_3Cl$. *Anal.* Calcd. for $C_{14}H_{16}N_3Cl$: C, 64.24; H, 6.16; N, 16.05; Found: C, 64.04; H, 6.38; N, 16.24.

***4-(5-(2,6-Dichlorophenyl)-1H-*pyrazol-3-yl)piperidine (3f).** White solid, mp 148–152°C; yield 84%; reaction time 1 h and 30 min. ^1H NMR (400 MHz, $CDCl_3$): δ 1.66–1.76

(2H, m, CH_2); 1.97–2.01 (2H, m, CH_2); 2.79–2.87 (3H, m, CH,CH_2); 3.18–3.21 (2H, m, CH_2); 6.40 (1H, s, pyrazol proton); 7.33–7.35 (1H, m, ArH, J = 8.4 Hz,); 7.39–7.43 (1H, d, J = 8.4 Hz, ArH); 7.73–7.75 (1H, m, ArH). ^{13}C NMR (100 MHz, $CDCl_3$): δ 33.1, 34.7, 46.5, 99.5, 125.6, 127.8, 128.7, 132.4, 149.3, 152.5. IR (KBr, cm^{-1}): 3237, 3236, 1646, 1320, 1295, 1079. ESI/MS 296.1 $[M]^+$, 298.2 $[M+2]^+$, 300.1 $[M+4]^+$ calculated for $C_{14}H_{15}N_3Cl_2$. *Anal.* Calcd. for $C_{14}H_{15}N_3Cl_2$: C, 56.77; H, 5.10; N, 14.19; Found: C, 56.63; H, 5.45; N, 14.35.

***4-(5-(3-Bromophenyl)-1H*-pyrazol-3-yl)piperidine (3g)**. White solid, mp 152–156°C; yield 62%; reaction time 20 min. ^{1}H NMR (400 MHz, $CDCl_3$): δ 1.69–1.79 (2H, m, CH_2); 1.99–2.02 (2H, m, CH_2); 2.74–2.80 (2H, m, CH); 2.82–2.88 (1H, m, CH); 3.20–3.23 (2H, d, CH_2); 6.39 (1H, s, pyrazol proton); 6.99–7.04 (1H, m, ArH, J = 8.4 Hz); 7.36–7.40 (1H, m, ArH, J = 8.4 Hz,); 7.45–7.48 (1H, m, J = 8.4 Hz, ArH); 7.52–7.54 (1H, m, ArH,). ^{13}CNMR (100 MHz, $CDCl_3$): δ 33.1, 34.4, 46.4, 99.8, 112.3, 112.6, 114.5, 114.7, 121.2, 130.1, 130.2, 130.3, 135.1. IR (KBr, cm^{-1}): 3336, 3079, 2996, 2953, 2817, 1360, 1287, 1119. ESI/MS 306.1 $[M]^+$, 308.1 $[M+2]^+$ calculated for $C_{14}H_{16}N_3Br$. *Anal.* Calcd. for $C_{14}H_{16}N_3Br$: C, 54.91; H, 5.27; N, 26.10; Found: C, 55.00; H, 5.38; N, 13.64.

***4-(5-(4-Fluorophenyl)-1H*-pyrazol-3-yl)piperidine (3h)**. White solid, mp 181–184°C; yield 67%; reaction time 15 min. ^{1}H NMR (400 MHz, $CDCl_3$): δ 1.68–1.79 (2H, m, CH_2); 1.99–2.02 (2H, m, CH_2); 2.73–2.81 (2H, m, CH); 2.82–2.89 (1H, m, CH); 3.20–3.23 (2H, m, CH_2); 6.34 (1H, s, pyrazol proton); 7.07–7.12 (2H, m, ArH); 7.70–7.73 (2H, m, ArH). ^{13}C NMR (100 MHz, $CDCl_3$): δ 33.0, 34.5, 46.4, 99.41, 115.5, 115.7, 127.2, 127.3, 151.7, 161.3, 163.7. IR (KBr, cm^{-1}): 3246, 2950, 2830, 1363, 1264, 1095, 1006. ESI/MS 246.2 $[M+1]^+$ calculated for $C_{14}H_{16}N_3F$. *Anal.* Calcd. for $C_{14}H_{16}N_3F$: C, 68.55; H, 6.57; N, 17.13; Found: C, 68.79; H, 6.73; N, 17.25.

***4-(5-(3-Fluoro-4-methoxyphenyl)-1H*-pyrazol-3-yl)piperidine (3i)**. White solid, mp 142–144°C; yield 74%; reaction time 45 min. ^{1}H NMR (400 MHz, $CDCl_3$): δ 1.69–1.77 (2H, m, CH_2); 1.96–2.00 (2H, m, CH_2); 2.71–2.75 (2H, m, CH_2); 2.77–2.85 (1H, m, CH); 3.18–3.21 (2H, m, CH_2); 3.92 (3H, S, OCH_3); 6.30 (1H, s, pyrazol proton); 6.96–7.00 (1H, t, ArH, J = 8.8, 8.4 Hz,); 7.45–7.50 (2H, m, ArH). ^{13}C NMR (100 MHz, $CDCl_3$): δ 32.9, 34.5, 46.5, 56.3, 99.3, 105.4, 113.4, 113.6, 121.3, 121.4, 147.3, 151.2, 153.7. IR (KBr, cm^{-1}): 3335, 2945, 2842, 1364, 1270. ESI/MS 276.1 $[M+1]^+$ calculated for $C_{15}H_{18}N_3FO$. *Anal.* Calcd. for $C_{15}H_{18}N_3FO$: C, 65.44; H, 6.59; N, 15.26; Found: C, 65.57; H, 6.51; N, 15.42.

***4-(3-(Piperidin-4-yl)-1H*-pyrazol-5-yl)benzonitrile (3j)**. White solid, mp 168–170°C; yield 76%; reaction time 40 min. ^{1}H NMR (400 MHz, $CDCl_3$): δ 1.71–1.79 (2H, m, CH_2); 2.00–2.02 (2H, m, CH_2); 2.75–2.90 (3H, m, CH, CH_2); 3.21–3.24 (2H, m, CH_2); 6.46 (1H, s, pyrazol proton); 7.69–7.71 (2H, m, ArH, J = 8.4 Hz,); 7.88–7.90 (2H, d, J = 8.4 Hz, ArH). ^{13}C NMR (100 MHz, DMSO): δ 33.0, 34.2, 46.3, 100.2, 109.7, 119.5, 125.9, 133.1, 138.4, 147.9, 151.4. IR (KBr, cm^{-1}): 3355, 3068, 2265, 1364, 1265, 1004, 907. ESI/MS 253.2 $[M+1]^+$ calculated for $C_{15}H_{16}N_4$. *Anal.* Calcd. for $C_{15}H_{16}N_4$: C, 71.40; H, 6.39; N, 22.21; Found: C, 71.17; H, 6.55; N, 22.28.

***4-(5-(4-Tolyl)-1H*-pyrazol-3-yl)piperidine (3k)**. White solid, mp 158–161°C; yield 62%; reaction time 1 h. ^{1}H NMR (400 MHz, $CDCl_3$): δ 1.68–1.76 (2H, m, CH_2); 1.97–2.00 (2H, m, CH_2); 2.38 (3H, s, CH_3); 2.69–2.77 (1H, m, CH); 2.79–2.85(2H, m, CH_2); 3.18–3.02 (2H, m, CH_2); 6.34 (1H, s, pyrazol proton); 7.20–7.22 (2H, m, ArH, J = 8.4 Hz,); 7.59–7.61 (2H, d, J = 8.4 Hz, ArH). ^{13}C NMR (100 MHz, $CDCl_3$): δ 21.3, 33.1, 34.8, 46.5, 99.3, 125.5, 129.4, 137.7, 148.9, 152.8. IR (KBr, cm^{-1}): 3248, 3068, 1361, 1265, 1004, 907. ESI/MS 242.2 $[M+1]^+$ calculated for $C_{15}H_{19}N_3$. *Anal.* Calcd. for $C_{15}H_{19}N_3$: C, 74.65; H, 7.94; N, 17.41; Found: C, 74.93; H, 7.76; N, 17.31.

***3-Chloro-4-(3-(piperidin-4-yl)-1H*-pyrazol-5-yl)pyridine (3l)**. White solid, mp 176–179°C; yield 48%; reaction time 10 min. ^{1}H NMR (400 MHz, DMSO): δ 1.47–1.57 (2H, m, CH_2); 1.84–1.87 (2H, m, CH_2); 2.54–2.60 (2H, m, CH_2); 2.74–2.80 (1H, m, CH); 2.98–3.01 (2H, m, CH_2); 6.72 (1H, s, pyrazol proton); 7.84–7.85 (1H, d, ArH, J = 6 Hz,); 8.49–8.50 (1H, d, J = 6.4 Hz, ArH); 8.65 (1H, s, ArH); 13.1 (1H, b, NH, piperidine). ^{13}C NMR (100 MHz, $CDCl_3$): δ 33.0, 34.2, 46.3, 100.2, 119.8, 141.2, 141.6, 147.0, 147.5, 150.4. IR (KBr, cm^{-1}): 3339, 3068, 1364, 1265, 1004, 907. ESI/MS 263.0 $[M]^+$, 265.1 $[M+2]^+$ calculated for $C_{13}H_{15}ClN_4$. *Anal.* Calcd. for $C_{13}H_{15}ClN_4$: C, 59.43; H, 5.75; N, 21.32; Found: C, 59.19; H, 5.97; N, 21.19.

***4-(5-(3-Nitrophenyl)-1H*-pyrazol-3-yl)piperidine (3m)**. Yellow solid, mp 158–161°C; yield 65%; reaction time 1 h and 45 min. ^{1}H NMR (400 MHz, $CDCl_3$): δ 1.75–1.82 (2H, m, CH_2); 1.99–2.03 (2H, m, CH_2); 2.73–2.77 (2H, m, CH_2); 2.79–2.80 (1H, m, CH); 3.20–3.23 (2H, m, CH_2); 6.43 (1H, s, pyrazol proton); 7.59–7.55 (1H, m, ArH); 8.01–8.10 (1H, d, J = 8.4 Hz, ArH); 8.22–8.24 (1H, m, ArH, J = 8.4 Hz,); 8.56–8.61 (1H, m, ArH, J = 8.4 Hz). ^{13}C NMR (100 MHz, DMSO): δ 33.1, 34.7, 46.5, 99.5, 125.6, 127.8, 128.7, 132.4, 149.3, 152.5. IR (KBr, cm^{-1}): 3326, 3002, 2267, 1531, 2217, 1348. ESI/MS 273.0 $[M+1]^+$ calculated for $C_{14}H_{16}N_4O_2$. *Anal.* Calcd. for $C_{14}H_{16}N_4O_2$: C, 61.75; H, 5.92; N, 20.58; Found: C, 61.59; H, 6.04; N, 20.51.

***4-(5-(2-Nitrophenyl)-1H*-pyrazol-3-yl)piperidine (3n)**. Yellow solid, mp 140–142°C; yield 67%; reaction time 3 h. ^{1}H NMR (400 MHz, $CDCl_3$): δ 1.74–1.80 (2H, m, CH_2); 2.00–2.03 (2H, m, CH_2); 2.74–2.78 (2H, m, CH_2); 2.80–2.83 (1H, m, CH); 3.20–3.23 (2H, m, CH_2); 6.48 (1H, s, pyrazol proton); 7.60–7.68 (1H, m, ArH); 7.89–7.92 (1H, m, ArH,) 8.00–8.20

(2H, m, ArH). ^{13}C NMR (100 MHz, DMSO): δ 21.2, 29.0, 35.1, 101.2, 124.4, 125.3, 129.6, 132.4, 135.3, 148.3, 157.0 152.5. IR (KBr, cm^{-1}): 3320, 3006, 2258, 2223, 1534, 1344. ESI/MS 273.0 $[M+1]^+$ calculated for $C_{14}H_{16}N_4O_2$. *Anal.* Calcd. for $C_{14}H_{16}N_4O_2$: C, 61.75; H, 5.92; N, 20.58; Found: C, 61.65; H, 6.09; N, 20.79.

STATISTICAL ANALYSIS

Calculations and statistics were performed using graph pad Prism 3.02 software. Data was expressed as mean ± standard error.

Acknowledgments. The authors are grateful to the Synth Services Pvt. Ltd, Jarod, Vadodara, India, for financial assistance.

REFERENCES AND NOTES

[1] Yusuf, S.; Reddy, S.; Ounpuu, S. Circulation 2001, 104, 2746.
[2] Fitzgerald, D. J. Neurology 2001, 57, S1.
[3] World Health Organization (WHO) http://www.who.int/cardiovascular_diseases/en/. Accessed in 2008.
[4] Makin, A.; Silverman, S. H.; Lip, G. Y. H Q J Med 2002, 95, 199.
[5] Bhatt, D. L.; Topol, E. J Med Clin North Am 2000, 84, 163.
[6] Easton, J. D. Cerebrovasc Dis 2001, 11, 23.
[7] Antithrombotic Trialists' Collaboration BMJ 2002, 324, 71.
[8] Bruno, O.; Brullo, C.; Schenone, S.; Bondavalli, F.; Ranise, A.; Tognolini, M.; Impicciatore, M.; Ballabeni, V.; Barocelli, E. Bioorg Med Chem 2006, 14, 121.
[9] Cattaneo, M. Hematol J 2004, 5, S170.
[10] Parekh, P. J.; Oldfield, E. C. IV; Johnson, D. A. Drugs 2015, 75, 1613.
[11] Cattaneo, M. Arterioscler Thromb Vasc Biol 2004, 24, 1980.
[12] Patrono, C. J. Thromb Haemost 2003, 1, 1710.
[13] Campbell, C. L.; Steinhubl, S. R.; Campbell, C. L. J Thromb Haemost 2005, 3, 665.
[14] Giridhar, R.; Tamboli, R. S.; Ramajayam, R.; Prajapati, D. G.; Yadav, M. R. Eur J Med Chem 2012, 50, 428.
[15] Arias, H. R.; López, J. J.; Feuerbach, D.; Fierro, A.; Ortells, M. O.; Pérez, E. G. Int J Biochem Cell Biol 2013, 45, 2420.
[16] Rodríguez-Franco, M. I.; Dorronsoro, I.; Castro, A.; Martínez, A.; Badía, A.; Baños, J. E. Bioorg Med Chem 2003, 10, 2263.
[17] Farnell, L.; Ganellin, C. R.; Durant, G. J.; Parsons, E.; Ganellin, C. R.; Port, J.; Richards, W. G.; Ganellin, R.; Ganellin, C. R.; Black, W.; Pullman, H.; Port, J.; Kakudo, M.; Aschman, D. H.; Black, J. W. J Med Chem 1975, 18, 666.
[18] Soni, J. Y.; Premasagar, V.; Thakore, S. I. Lett Org Chem 2015, 15, 277.
[19] Soni, J. Y.; Sanghvi, S.; Devkar, R. V.; Thakore, S. I. RSC Advances 2015, 5, 82112.
[20] Rowley, M.; Collins, I.; Broughton, H. B.; Davey, W. B.; Baker, R.; Emms, F.; Marwood, R.; Patel, S.; Ragan, C. I.; Freedman, S. B.; Ball, R.; Leeson, P. D. J Med Chem 1997, 40, 2374.
[21] Mazurov, A.; Klucik, J.; Miao, L.; Phillips, T. Y.; Seamans, A.; Schmitt, J. D.; Hauser, T. A.; Johnson, R. T.; Miller, C. Bioorg Med Chem Lett 2005, 15, 2073.
[22] Gorbyleva, O. I.; Filipenko, T. Y.; Mikhlina, E. E.; Turchin, K. F.; Sheinker, Y. N.; Yakhontov, L. N. Chem Heterocycl Compd 1982, 18, 601.
[23] Warawa, E. J.; Mueller, N. J.; Gylys, J. A. J Med Chem 1975, 18, 71.
[24] Coffen, D. L.; Katonak, D. A.; Wong, F. J Am Chem Soc 1974, 96, 3966.
[25] Davis, B. N.; Abelt, C. J. J Phys Chem A 2005, 109, 1295.
[26] Sonar, V. N.; Venkataraj, M.; Parkin, S.; Crooks, P. Acta Crystallogr Sect E Struct Reports Online 2006, 62, 05576.
[27] Liming, H.; Fu, Y.; Li, H. J.; Early, Z. C. CN 101812054B 2010.

RSC Advances

PAPER

View Article Online
View Journal | View Issue

Cite this: *RSC Adv.*, 2015, **5**, 82112

Synthesis and evaluation of novel quinuclidinone derivatives as potential anti-proliferative agents†

Jigar Y. Soni,[a] Shridhar Sanghvi,[b] R. V. Devkar[b] and Sonal Thakore*[a]

Received 29th July 2015
Accepted 18th September 2015

DOI: 10.1039/c5ra15127a

www.rsc.org/advances

In this study a new series of substituted (*Z*)-4-(3-oxoquinuclidin-2-ylidene) benzamides and substituted (*Z*)-4-((3-oxoquinuclidin-2-ylidene)methyl)benzoates have been designed and synthesised as potential anti-cancer agents. This set of compounds were prepared by using a common intermediate (*Z*)-4-((3-oxoquinuclidin-2-ylidene)methyl)benzoic acid. They were well characterized by various spectroscopic techniques as well as a crystallographic study and screened for anti-cancer activity. A cell viability assay using MTT was performed on A549 & L132 cell lines and IC_{50} values were determined. Analogues **4c** and **5e** exhibited the most potent anti-cancer activity among all the analogues synthesized in this present study. A haemolytic assay using normal human erythrocytes was performed to study the blood compatibility of the compounds. Acridine orange/ethidium bromide (AO/EB) staining also showed cell death. To get a better insight into the mechanism of cell death DAPI (4′,6-diamido-2-phenylindol nuclear staining) and DNA fragmentation studies were performed. A Structure Activity Relationship (SAR) was explored to facilitate further development of this new class of compounds.

1 Introduction

Cancer, a serious health problem, is one of the main causes of mortality in the developing as well as developed countries.[1] Different theories have been proposed for the cause of cancer and several strategies have been formulated and examined for combating the disease. Survival rates for five years of some cancers have significantly improved in the past two decades while those of other cancers, such as lung and pancreatic cancer remain low.[2] The major form of cancer treatment is chemotherapy, alone or combined with radiation. However, the majority of cancers develop resistance to chemotherapy during treatment. As a result, the design and discovery of non-traditional, efficient and safe classes of chemical agents are the prime targets in contemporary medicinal chemistry.[3]

The molecule 3-quinuclidinone hydrochloride possesses variety of biological spectrum and is a part of many existing drugs such as azasetron, palonosetron, solifenacin, cevimeline, quinupramine (Fig. 1). Literature survey revealed that several derivatives of quinuclidines have been reported to show wide range of biological activity such as Alzheimer's disease[4] chronic obstructive pulmonary disease,[5] antihistamine-bronchodilating agents,[6] α7 and α4β2 nicotinic receptors inhibitory activity.[7] According to Malki *et al.* analogs of quinuclidinone can provide an excellent scaffold for novel anti-cancer agents with improved safety profile.[8] They used lung carcinoma cells for study and observed that in more potent derivatives, the carbonyl group of quinuclidinone was intact.[8] Further in another study they observed that quinuclidinone derivatives induce apoptosis in human breast cancer cells *via* reduced expression level of Bcl-2, Bcl-XL and increased mitochondrial apoptotic pathways by activating the release of cytochrome C.[9] The derivatives of this molecule may have a selective mode of action as they are structurally unique, and yet have a great deal of known chemistry upon which to prepare analogs. In search of novel more potent anti-cancer compounds with greater affinity for cancer cells than healthy normal cells, we decided to explore the anti-cancer activity of some novel quinuclidinone derivatives. We have recently reported the synthesis of quinuclidinone hydrochloride from isonipecotic acid.[10] In the present article we report the synthesis of some quinuclidinone based ester and amide derivatives with cytotoxicity and apoptosis-inducing property in lung cancer cells.

2 Result and discussion

2.1 Synthesis

In the first step 3-quinuclidinone hydrochloride (**1**) was refluxed with 4-formyl benzoic acid (**2**) in the presence of sodium hydroxide, using absolute ethanol as solvent to give 4-(3-oxo-1-aza-bicyclo[2.2.2]oct-2-ylidenemethyl)-benzoic acid (**3**) (Scheme 1).

[a]*Department of Chemistry, Faculty of Science, The M. S. University of Baroda, Vadodara, 390 002, India. E-mail: chemistry2797@yahoo.com; Tel: +91-0265-2795552*

[b]*Department of Zoology, Faculty of Science, The M. S. University of Baroda, Vadodara, 390 001, India*

† Electronic supplementary information (ESI) available. CCDC 1025491 and 1051487 contains the crystallographic data for the compounds **4c** and **5c** respectively. For ESI and crystallographic data in CIF or other electronic format see DOI: 10.1039/c5ra15127a

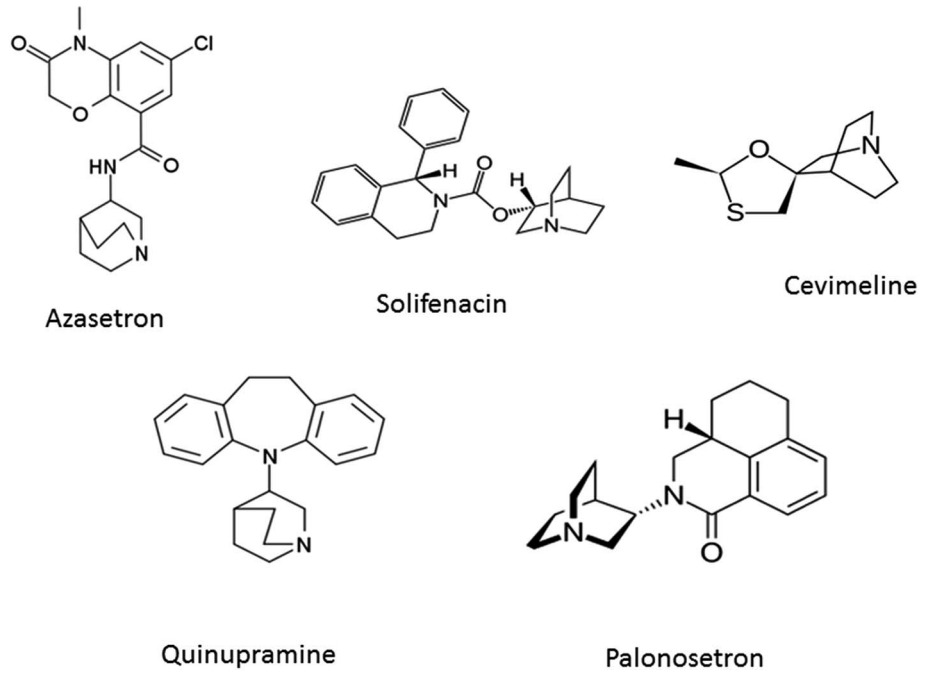

Fig. 1 Structures of some quinuclidine based drugs.

Formation of this intermediate acid (**3**) was confirmed from the broad absorption band at around 3200 cm^{-1} in the infrared spectrum (IR) and downfield peak at 13.1 δ ppm in ^1H NMR. The acid derivative (**3**) was converted to the acid chloride with thionyl chloride in the presence of triethylamine. The acid chloride was further converted in to the corresponding ester or amide derivative by reaction with appropriate alcohol/amine. The structure of synthesized compounds established on the basis of elemental analysis and spectral data. In case of amide derivatives (**4a** to **4f**), the NH stretching frequency appeared around 3300 to 3450 cm^{-1}. The formation of ester (**5a** to **5e**) was confirmed from the disappearance of the broadband of carboxyl in the IR spectrum and appearance of absorption band in the region 1728–1750 cm^{-1}. ^{13}C NMR downfield peak appeared around 165–169 δ ppm, which further confirms the formation of ester derivatives. Single crystal of compound **4c** and **5c** (Fig. 6 and 7) were obtained by slow evaporation method using methanol as a solvent. The crystal structures of compound **4c** and **5c** shows the presence of double bond with *Z* geometry. This is well in agreement with previous report.[11]

2.2 Biological assay and structure activity relationship (SAR)

The synthesized compounds were screened for MTT assay. All compounds were screened at 1, 5, 10 and 20 μM concentrations. The results obtained in a cytotoxicity assay for quinuclidinone and its ester and amide analogues accounted for decreased cell viability in a dose dependent manner. The results also suggest

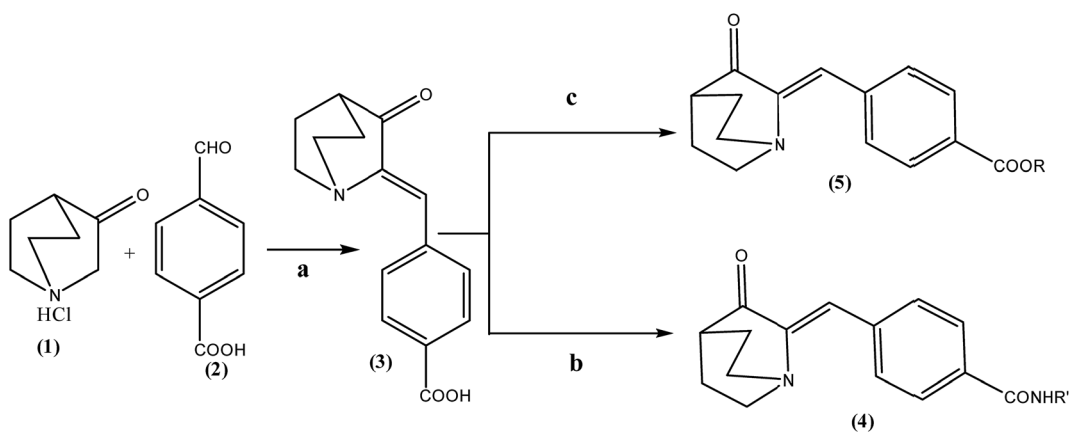

Scheme 1 Synthetic route for compounds (4) and (5); (reagents and conditions: (a) NaOH, EtOH, reflux; (b) (1) MDC, TEA, $SOCl_2$, reflux; (2) R′–NH_2, ACN, K_2CO_3, reflux; (c) (1) MDC, TEA, $SOCl_2$, reflux; (2) R–OH reflux).

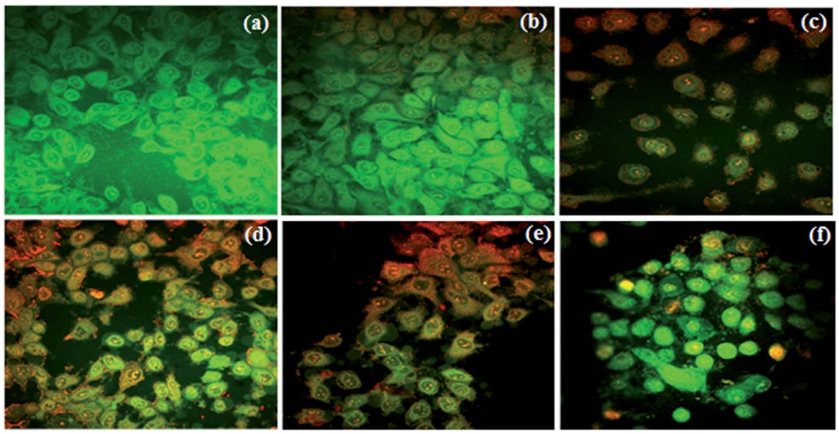

Fig. 2 Photomicrographs ofAO/EB staining for apoptosis, treated with (a) control, compounds (b) **4c**, (c) **4d**, (d) **5c**, (e) **5d** and (f) **1** respectively at their IC_{50} values for 24 h (green fluorescence indicated live cells whereas reddish orange stained cells indicate late apoptosis).

that the synthesized compounds showed specificity for cancer cells over normal lung cells.

The half inhibitory concentration IC_{50} values in μM concentration were determined and presented in Table 1. The results indicate that compared to esters all amide derivative exhibited reasonably good activity. Among amides the derivative having unsubstituted phenyl ring (**4a**) was found to be less active among all. The introduction of either electron donating group (methyl) or electron withdrawing group (bromo) increases the activity. Amide derivative having *para*-bromophenyl group (**4c**) was found to be most potent among all aromatic amides. In order to determine if aromatic ring is essential for activity, derivatives with cyclohexyl (**4d**) and heterocyclic ring such as morpholine (**4e**) and pyrrolidine (**4f**) were synthesized. In all these cases an increase in the activity was observed.

In ester series the derivatives in which the oxygen of ester group was attached to a secondary carbon exhibited better activity. Thus esters of secondary alcohols such as isopropyl alcohol, *sec*-butanol, and cyclopropyl alcohol were found to be more active. The compound (**5c**) bearing isopropyl group was found to be most active followed by (**5d**) and (**5e**) which were moderately active. Lowering of activity was observed when methyl (**5a**) and ethyl groups (**5b**) were introduced.

Synthesis of new chemotherapeutic agents with selective cytotoxicity towards cancer cells is always a major challenge for chemists and biotechnologists. Based upon the results obtained in the cytotoxicity assay the derivatives **4c**, **4e**, **5c** and **5d** were selected for a detailed scrutiny to assess the mode of cell death.

Cancer cells were stained with fluorescent stains to gain a deeper insight into the mechanism of cell death. Induction of apoptosis is a key event and a preferred pathway for induction of cell death by a test compound.[12] Hence, a fluorescent probe (AO/EB) was used to gather qualitative evidence on apoptosis. It has been reported that the viable cells show green fluorescence and late apoptotic cells show orange to red fluorescence with condensed chromatin.[13] We could observe more orange to red fluorescent cells **4c**, **4e** and **5c** as compared to **5d** and quinuclidinone HCl **1** treated cells suggesting induction of apoptosis (Fig. 2).

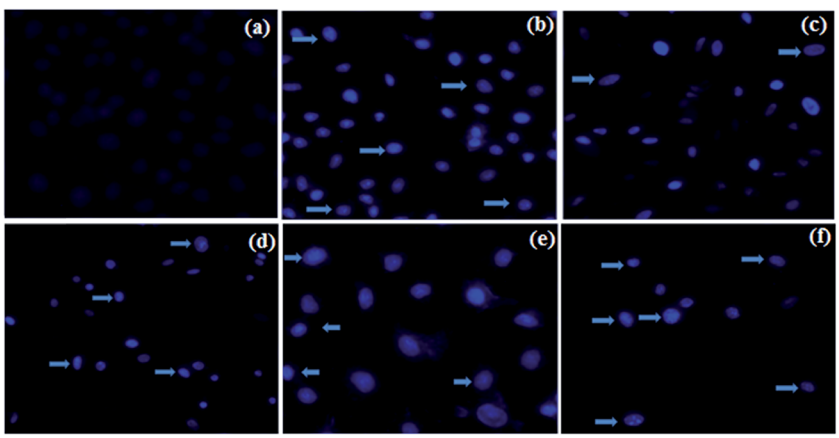

Fig. 3 Nuclear condensation test with DAPI for treated with (a) control, compounds (a) **4c**, (b) **4d**, (c) **5c**, (d) **5d** and (f) **1** respectively at their IC_{50} values for 24 h (arrows indicate condensation/fragmentation/distortion of nuclei as compared to the control).

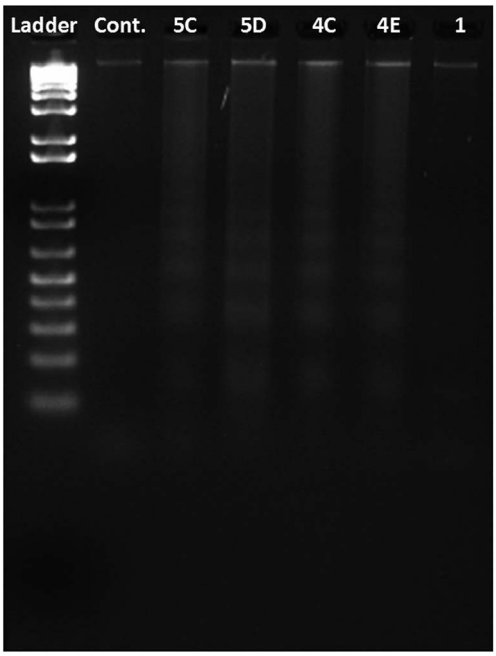

Fig. 4 DNA ladder test for apoptosis: ladder formation suggests induction of apoptosis (lane 1: ladder, lane 2: control, lane 3: **5d**, lane 4: **5c**, lane 5: **4c**, lane 6: **4e**, lane 7: quinuclidinone HCl **1**).

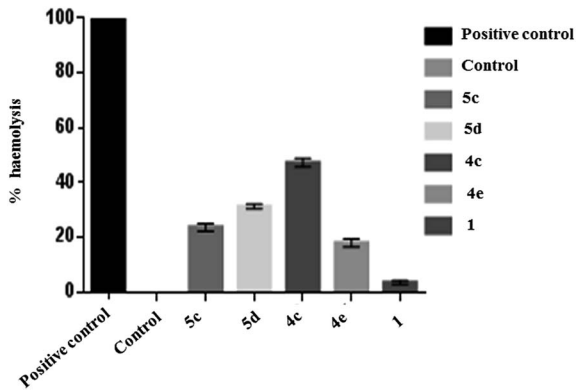

Fig. 5 Haemolysis of RBC.

Nuclear condensation resulting due to any test compound is assessed using DAPI staining.[14] In our study, condensation/fragmentation/distortion of nuclei was evident in all treatment groups (Fig. 3). Further confirmation on apoptosis was obtained from DNA ladder assay, wherein apoptosis induced DNA damage is accredited to possible induction of apoptotic pathway.[15] In the present study, all the test compounds showed moderate to heavy ladder formation (Fig. 4) suggesting induction of apoptosis.

Novel compounds that may be potent in destruction of cancer cells often cause damage to the red blood corpuscles (RBC) and hence, haemolytic assay provides a clue on its merit in not destroying the RBC.[16] Hence, haemolytic assay is a popular tool to assess the relative impact of test compounds on RBCs.[16] In our study **4e**, **5e**, **5f**, and the quinuclidinoneHCl **1** accounted for moderate haemolysis indicating at their relative safety for *in vivo* use as a possible therapeutant (Fig. 5).

3 Conclusions

In conclusion a series of novel quinuclidinone based amides and esters (**4a** to **4f** and **5a** to **5f**) were synthesized. The structures of title compounds were well supported by spectroscopic data and elemental analysis. Test compounds were able to induce apoptosis of A549 lung carcinoma cells with minimal damage to the L132 normal lung cells. The most potent compounds (**4c**, **4e**, **5c** and **5d**) were subjected to further investigations. DNA fragmentation suggests that the cytotoxic effect of the compound is selectively mediated through the induction of apoptosis. Additional experiments are required to determine the mechanism of action and for better elucidation of structure activity relationships of this class of molecules.

4 Experimental

4.1 Materials and methods

Commercial grade solvents and reagents (alcohols and amines) were purchased from Sigma-Aldrich or Alfa Aeser or Spectrochem, Mumbai, India and used without further purification. Quinuclidinone hydrochloride was prepared as described in literature.[10] Melting points were measured using a (Buchi B-545) melting point apparatus and were uncorrected. Infrared spectra were recorded on a Perkin-Elmer RX 1 spectrometer. Elemental analyses were recorded on Thermo Finnigan Flash 11-12 series EA. ^{1}H and ^{13}C NMR spectra were recorded on an Advance Bruker (400 MHz) spectrometer in suitable deuterated solvents. ^{1}HNMR data were recorded as follows: chemical shift measured in parts per million (ppm) downfield from TMS multiplicity, observed coupling constant (*J*) in Hertz (Hz), proton count. Multiplicities are reported as singlet (s), broad singlet (br s), doublet (d), triplet (t), quartet (q) and multiplet (m). ^{13}C NMR chemical shifts are reported in ppm downfield from TMS. Solvents and reagents were purified by literature methods. Mass spectra were determined by LC/MS, using Shimadzu LCMS 2020 and AB Sciex 3200 QTRAP. The reaction progress was monitored by TLC in ultraviolet light as well as with iodine vapor.

4.2 Biological assay

4.2.1 Cell line and culture. The A549 and L132 cell lines were obtained from the National Center for Cell Sciences, Pune whereas Dubecoos Modified Essential Medium (DMEM), Fetus Bovine Serum (FBS) and antimycotic–antibiotic solution were obtained from HiMedia. The human cell lines A549 and L132 were seeded in T-25 flask with DMEM, 10% FBS and 1% antimycotic–antibody solution in a humidified atmosphere supplied with 5% CO_2 at 37 °C. Cells were subsequently subcultured every third day by trypsinization with 0.25% trypsin *versus* glucose solution. Both the cell lines were utilized to examine the antitumor activity of testing compound at varying concentration.

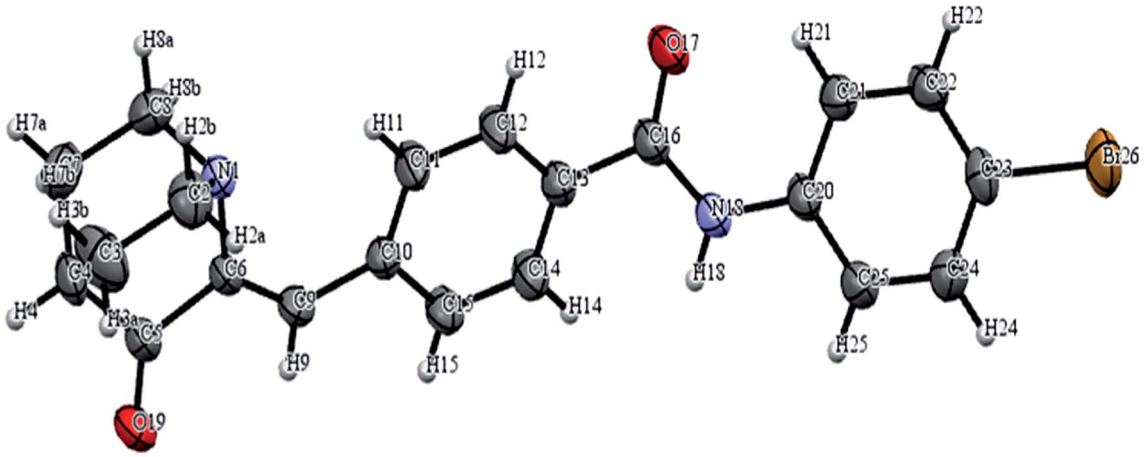

Fig. 6 ORTEP diagram of compound **4c** with atom numbering scheme. Displacement ellipsoids are drawn at the 50% probability.

4.2.2 Cell viability assay. The IC_{50} values of cell proliferation were determined using MTT assay. Quinuclidinone and its derivatives were dissolved in 0.5% dimethyl sulfoxide and subsequent doses were prepared in the media. A549 cells were seeded in 96 well culture plates and were treated with different concentrations of the compounds for 24 h. The positive control cells were treated with quinuclidinone in culture medium at subsequent doses. At the end of the incubation period 100 μl of 3-(4,5-dimethylthiazol-2-yl)-2,5-diphenyltetrazolium bromide (MTT; 1 mg ml^{-1}) was added to the wells and plates were incubated at 37 °C for 4 h. Later, culture medium was discarded and 150 μl DMSO was added. Absorbance was read at 540 nm in ELX800 Universal Microplate Reader.

4.2.3 Nuclear morphology assessment (DAPI staining). A549 cells were seeded in 6 well plate (5×10^5) and were allowed to achieve 80% confluence. Cells were treated with IC_{50} values of the compounds for 24 h at 37 °C. Cells were washed with PBS and fixed with 1% paraformaldehyde, rewashed with PBS and incubated with DAPI for 5 min. Treated cells were examined for condensed and fragmented nuclei and photographed under Leica DMRB fluorescence microscope.

4.2.4 Assessment of apoptosis AO/EtBr staining. Cells were grown on glass cover slip (5×10^6) and were incubated in a CO_2 incubator at 37 °C. Cells were dosed with IC_{50} concentration of compounds. After 24 h incubation, cells were washed with PBS and stained with 5 μl of AO–EtBr mixture. The coverslip was placed on clean microscopic slides and photograph was taken under confocal microscope (Carl Zeiss LSM-710).

4.2.5 Haemolytic assay. Whole blood was collected for haemolytic assay from a healthy human volunteer after taking a written consent. Protocol was approved and experiments were performed in compliance with the relevant laws and guidelines of Indian medical association for research on human subjects at Blue cross pathology lab (IMA-BMWMC no. 1093), Vadodara,

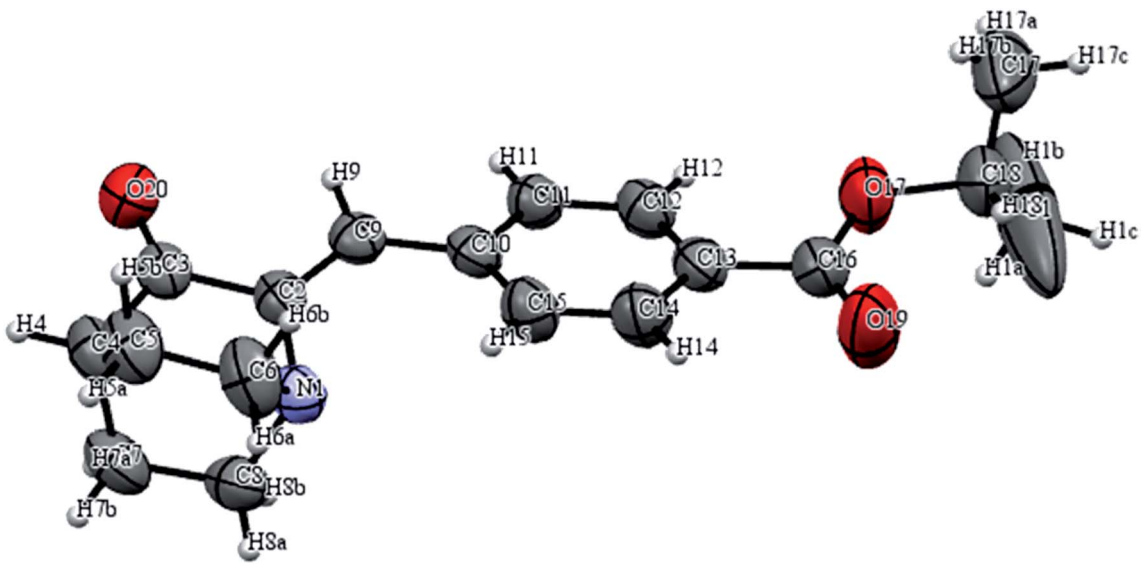

Fig. 7 ORTEP diagram of compound **5c** with atom numbering scheme. Displacement ellipsoids are drawn at the 50% probability.

Table 1 IC_{50} values of the compounds 4(a–f) and 5(a–e)

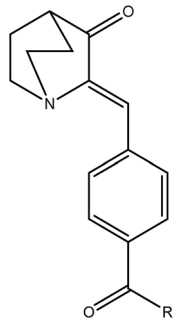

Compound	Structure	IC_{50} (μM)	Compound	Structure	IC_{50} (μM)
4a	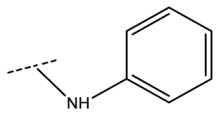	3.26 ± 1.4	**5a**	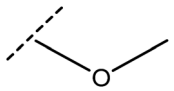	9.22 ± 1.2
4b	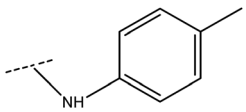	1.24 ± 0.5	**5b**	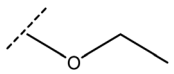	8.77 ± 0.6
4c	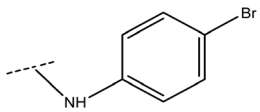	0.225 ± 0.7	**5c**	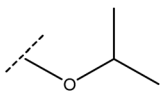	1.5 ± 0.9
4d	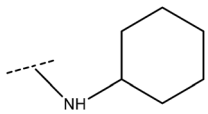	1.301 ± 0.4	**5d**	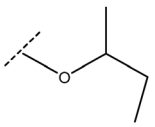	5.74 ± 0.8
4e	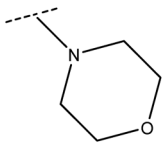	0.665 ± S1.4	**5e**	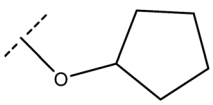	6.15 ± 1.0
4f	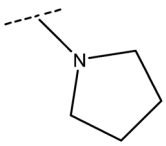	1.24 ± 0.9			

India. The blood samples were placed in vacutainer tubes coated with ethylenediaminetetra-acetic acid (EDTA) and were gently mixed and treated with IC_{50} concentration of the compounds. Control was untreated (with 0% haemolysis) and positive control was sample treated with 3% hydrogen peroxide (with 100% haemolysis). After incubation for 3 h (an adjustment of the standard ASTM F-756 (ref. 17)) the tubes containing blood samples were centrifuged at 1500 rpm for 10 min to collect the plasma. The supernatant was analysed for the presence of the haemoglobin at 540 nm and percentage haemolysis calculated according to the procedure described by Shiny *et al.*[18]

4.2.6 DNA ladder assay. A549 cells (3×10^6) were exposed to the IC_{50} concentration of the compounds. Cells were centrifuged and then washed with PBS, and the pellet was lysed with 400 μL hypotonic buffer solution (containing 10 mM of tris (pH 7.5), 1 mM of EDTA and 0.2% triton X-100) for 15 min at room temperature, and then centrifuged at 13 000 rpm for 15 min. 350 μL of the supernatant was again lysed in 106 μL of second lysis buffer (150 mM NaCl, 10 mM Tris–HCl (pH 8.0), 40 mM EDTA, 1% SDS and 0.2 mg mL^{-1} of proteinase K, at final concentration) for 4 h at 37 °C. The DNA was extracted with phenol/chloroform/isoamyl alcohol (25 : 25 : 1 v/v/v), and the pellet thus obtained was washed with ethanol and re-suspended for RNAase digestion in 15 μL of 10 mM Tris, 1 mM of EDTA (pH 8.5), and 50 μg mL^{-1} of RNAase for 1 h at 37 °C. The fragmented DNA was quantified on 2% agarose gel electrophoresis.[19]

4.3 Synthesis of (*Z*)-4-((3-oxoquinuclidin-2-ylidene)methyl) benzoic acid (3)

Compound **1** and formyl benzoic acid were taken in absolute ethanol and the solution was refluxed with catalytic amount of sodium hydroxide for about 3–4 h. The reaction progress was monitored by TLC. After completion the reaction mixture was acidified with glacial acetic acid. Crude product precipitated was filtered and washed with water. It was dried under vacuum and recrystallized using IPA-water.

4.4 General procedure for the preparation of compounds amides (4)

The product of step one (1 mmol) was taken in 20 ml dichloromethane and triethyl amine (3 mmol) was added. The resulting mixture was stirred at 0 °C and thionyl chloride (1.1 mmol) was added carefully. It was then warmed to room temperature and refluxed for 30 min. After solvent evaporation the unreacted thionyl chloride was removed under vacuum. The acid chloride thus obtained was taken in 20 ml acetonitrile and appropriate amine (1.12 mol) was added followed by K_2CO_3 (3 mmol). The reaction mixture was refluxed and the progress of the reaction was monitored by TLC. After completion, the alcohol was evaporated under vacuum. The residue was dissolved in ethyl acetate (50 ml) and washed with water and sat. $NaHCO_3$ solution. The organic layer was dried with sodium sulfate and solvent evaporated to give the ester as solid product.

4.5 General procedure for the preparation of esters (5)

To the acid chloride obtained above, appropriate alcohol was added in excess and the mixture was refluxed. The progress of the reaction was monitored by TLC. After completion, the alcohol was evaporated under vacuum. The residue was dissolved in ethyl acetate (50 ml) and washed with water and sat. $NaHCO_3$ solution. The organic layer was dried with sodium sulfate and solvent evaporated to give the ester as solid product.

4.5.1 (*Z*)-4-((3-Oxoquinuclidin-2-ylidene)methyl)benzoic acid (3). Yellow solid, mp: >250 °C; yield 78.6%. ^{1}H NMR (400 MHz, DMSO): δ ^{1}H NMR (400 MHz, DMSO): δ 1.88–1.94 (2H, m, –CH_2); 1.99–2.02 (2H, m, –CH_2); 2.49–2.50 (1H, m, –CH); 2.82–2.92 (2H, m, –CH_2); 3.12–3.25 (2H, m, –CH_2); 6.95 (1H, s, vinylic proton); 7.93–7.95 (2H, d, J = 8.0, –ArH); 8.14–8.16 (2H, d, J = 8.0, –ArH); 13.15 (1H, b, acid proton). ^{13}C NMR (100 MHz, DMSO): δ 25.3, 40, 47.3, 122.9, 129.6, 132.1, 137.7, 146.7, 167.5, 205.4. DEPT-135 (100 MHz, DMSO): δ 25.3, 40.0, 47.3, 122.8, 129.6, 132.1. IR (KBr, cm^{-1}): 3396, 2971, 2956, 2941, 2869, 1706, 1689, 1624, 1290, 805. ESI/MS 258.1 $[M + 1]^+$ calculated for $C_{15}H_{15}NO_3$. Anal. calcd for: C, 70.02; H, 5.88; N, 5.44; O, 18.65; found C, 70.42; H, 5.90; N, 5.38.

4.5.2 (*Z*)-4-((3-Oxoquinuclidin-2-ylidene)methyl)-*N*-phenylbenzamide (4a). Yellow solid, mp: 130–133 °C; yield 60%. ^{1}H NMR (400 MHz, DMSO): δ 2.00–2.03 (4H, m, 2-CH_2); 2.50–2.52 (1H, m, –CH); 2.86–2.91 (2H, m, –CH_2); 3.13–3.91 (2H, m, –CH_2); 6.98 (1H, s, vinylic proton); 7.08–7.12 (1H, t, J = 7.2, 14.2 Hz, –ArH), 7.33–7.37 (2H, t, J = 7.6, 15.6 Hz, –ArH); 7.77–7.79 (2H, d, J = 8 Hz, –ArH), 7.94–7.96 (2H, d, J = 8.4 Hz, –ArH); 8.17–8.19 (2H, d, J = 8.0 Hz, –ArH), 10.33 (1H, s, amide proton). ^{13}C NMR (100 MHz, DMSO): δ 25.3, 47.3, 114.3, 120.7, 123.0, 124.2, 128.1, 129.1, 129.2, 129.4, 131.5, 132.0, 135.8, 136.9, 139.5, 146.6, 165.5, 205.5. IR (KBr, cm^{-1}): 3388, 2960, 2943, 2869, 1699, 1656, 1597, 685. ESI/MS 333.2 $[M + 1]^+$ calculated for $C_{21}H_{20}N_2O_2$. Anal. calcd for: C, 75.88; H, 6.06; N, 8.43; O, 9.63; found C, 75.71; H, 6.27; N, 8.51.

4.5.3 (*Z*)-4-((3-Oxoquinuclidin-2-ylidene)methyl)-*N*-(*p*-tolyl) benzamide (4b). Yellow solid, mp: >250 °C; yield 58%. ^{1}H NMR (400 MHz, $CDCl_3$): δ 2.06–2.08 (4H, m, 2-CH_2); 2.36 (3H, s, –CH_3); 2.67–2.68 (1H, m, –CH), 2.99–3.05 (2H, m, –CH_2); 3.17–3.22 (2H, m, –CH_2); 7.04 (1H, s, vinylic proton); 7.18–7.02 (2H, d, J = 8.4 Hz, –ArH); 7.53–7.55 (2H, d, J = 8.0 Hz, –ArH); 7.85–7.87 (2H, d, J = 8.0 Hz, –ArH), 8.13–8.15 (2H, d, J = 8.4 Hz, –ArH). ^{13}C NMR (100 MHz, $CDCl_3$): δ 20.9, 25.7, 40.1, 47.4, 120.2, 123.6, 127.0, 129.6, 132.2, 134.3, 135.3, 137.1, 146.1, 165.1, 206.2. IR (KBr, cm^{-1}): 3295, 3130, 3042, 2950, 2869, 1703, 1644, 1607, 808. ESI/MS 347.2 $[M + 1]^+$ calculated for $C_{22}H_{22}N_2O_2$. Anal. calcd for: C, 76.28; H, 6.40; N, 8.09; O, 9.24; found C, 76.51; H, 6.26; N, 8.27.

4.5.4 (*Z*)-*N*-(4-Bromophenyl)-4-((3-oxoquinuclidin-2-ylidene) methyl)benzamide (4c). Yellow solid, mp: 207–208 °C; yield 69%. ^{1}H NMR (400 MHz, DMSO): δ 1.91–2.07 (4H, m, 2-CH_2); 2.85–2.92 (2H, m, –CH_2); 3.13–3.20 (2H, m, –CH_2); 6.98 (1H, s, vinylic proton); 7.53–7.55 (2H, d, J = 9.4 Hz, –ArH); 7.76–7.79 (2H, d, J = 9.2 Hz, –ArH); 7.94–7.96 (2H, d, J = 8.4 Hz, –ArH); 8.17–8.20 (2H, d, J = 8.4 Hz, –ArH); 10.50 (1H, s, amide). ^{13}C NMR (100 MHz, DMSO): δ 25.3, 47.3, 115.8, 122.6, 122.9, 128.1, 129.3, 131.9, 132.0, 135.5, 137.1, 139.0, 146.6, 165.6, 205.4. IR (KBr, cm^{-1}): 3373, 3302, 3086, 2942, 2866, 1698, 1677, 1620, 1588, 1466, 1067, 1036, 854. ESI/MS 410.2 $[M]^+$ calculated for $C_{21}H_{19}N_2BrO_2$. Anal. calcd for: C, 61.33; H, 4.66; N, 6.81; O, 7.78; Br, 19.43; found C, 61.47; H, 4.45; N, 6.97.

4.5.5 (*Z*)-*N*-Cyclohexyl-4-((3-oxoquinuclidin-2-ylidene)methyl) benzamide (4d). Yellow solid, mp: >225 °C; yield 73%. ^{1}H NMR (400 MHz, DMSO): δ 1.11–1.13 (1H, m, –CH_2); 1.24–1.35 (4H, m, 2-CH_2); 1.59–1.62 (1H, m, –CH_2); 1.72–1.73 (2H, m, –CH_2); 1.73–1.72 (2H, m, –CH_2); 1.86–1.92 (2H, m, –CH_2); 1.98–2.03 (2H, m, –CH_2); 2.83–2.90 (2H, m, –CH_2); 3.12–3.19 (2H, m, –CH_2); 3.73–3.75 (1H, m, –CH); 6.94 (1H, s, -vinylic proton); 7.81–7.83 (2H, d, J = 8.4 Hz, –ArH); 8.09–8.11 (2H, d, J = 8.4 Hz, –ArH); 8.22–8.24 (1H, d, amide).

^{13}C NMR (100 MHz, DMSO): δ 25.3, 32.8, 47.3, 48.8, 123.1, 127.7, 131.9, 135.7, 136.4, 146.35, 165.3, 205.4. IR (KBr, cm^{-1}): 3341, 2926, 2853, 1745, 1703, 1653, 1534, 1500, 800. ESI/MS 338.3 $[M + 1]^+$ calculated for $C_{21}H_{26}N_2O_2$.Anal. calcd for:: C, 74.53; H, 7.74; N, 8.28; O, 9.45; found C, 74.78; H, 7.51; N, 8.37.

4.5.6 (*Z*)-2-(4-(Morpholine-4-carbonyl)benzylidene)quinuclidin-3-one (4e). Yellow solid, mp: 155–156 °C; yield 55%. ^{1}H NMR (400 MHz, DMSO): δ 2.02–2.07 (4H, m, 2-CH_2); 2.65–2.66 (1H, m, –CH); 2.96–3.03 (2H, m, –CH_2); 3.15–3.22 (2H, m, –CH_2); 3.47–3.79 (8H, m, –4CH_2); 7.00 (1H, s, -vinylic proton); 7.40–7.42 (2H, d, J = 8.4 Hz, –ArH); 8.07–8.07 (2H, d, J = 8 Hz, –ArH). ^{13}C NMR (100 MHz, $CDCl_3$): δ 25.3, 40.1, 47.4, 51.6, 66.9, 123.8, 127.2, 132.1, 135.5, 135.8, 145.7, 169.9, 206.2. IR (KBr, cm^{-1}): 3444, 3027, 2962, 2869, 1707, 1683, 1635, 1438, 1110. ESI/MS 327.3 $[M + 1]^+$ calculated for $C_{15}H_{17}NO_2$. Anal. calcd for: C, 69.92; H, 6.79; N, 8.58; O, 14.71; C, 70.14; H, 6.51; N, 8.42.

4.5.7 (*Z*)-2-(4-(Pyrrolidine-1-carbonyl)benzylidene)quinuclidin-3-one (4f). Yellow solid, mp: 170–172 °C; yield 49%. ^{1}H NMR (400 MHz, $CDCl_3$): δ 1.90–1.96 (2H, m, $-CH_2$); 1.97–1.99 (2H, m, $-CH_2$); 2.01–2.07 (4H, m, 2-CH_2); 2.64–2.66 (1H, m, –CH); 2.96–3.03 (2H, m, $-CH_2$); 3.14–3.21 (2H, m, $-CH_2$); 3.42–3.46 (2H, t, $-CH_2$); 3.63–3.67 (2H, m, $-CH_2$); 7.00 (1H, s, -vinylic proton); 7.50–7.52 (2H, d, J = 8.4 Hz, –ArH); 8.05–8.07 (2H, d, J = 8.4 Hz, –ArH). ^{13}C NMR (100 MHz, $CDCl_3$): δ 24.4, 25.7, 26.4, 40.2, 46.2, 47.4, 49.5, 124.1, 127.1, 131.9, 135.3, 137.8, 145.5, 169.1, 206.3. IR (KBr, cm^{-1}): 3444, 2970, 2944, 2872, 1703, 1623, 1431, 1097. ESI/MS 311.4 $[M + 1]^+$ calculated for $C_{19}H_{22}N_2O_2$. Anal. calcd for: C, 73.52; H, 7.14; N, 9.03; O, 10.31; found C, 73.37; H, 7.29; N, 9.25.

4.5.8 Methyl(*Z*)-4-((3-oxoquinuclidin-2-ylidene)methyl)benzoate (5a). Yellow solid, mp: 142–143 °C; yield 70%. ^{1}H NMR (400 MHz, $CDCl_3$): δ 2.02–2.07 (4H, m, CH_2); 2.64–2.66 (1H, m, CH); 2.98–3.05 (2H, m, CH_2); 3.15–3.22 (2H, m, CH_2); 3.84 (3H, s, $-CH_3$); 6.90–6.93 (1H, dd, J = 4.0, 0.8 Hz, ArH), 7.00 (1H, s, vinylic proton); 7.28–7.32 (1H, t, J = 8.0, 7.6 Hz, ArH); 7.53–7.55 (1H, d, J = 7.2 Hz, ArH); 7.81 (1H, s, ArH). ^{13}C NMR (100 MHz, $CDCl_3$): δ 25.8, 40.2, 47.4, 51.2, 115.3, 117.0, 124.9, 125.0, 129.3, 135.2, 169.3, 206.5. IR (KBr, cm^{-1}): 3380, 3049, 2290, 2220, 2869, 1759, 1728, 1700, 1620. ESI/MS 272.2 $[M + 1]^+$ calculated for $C_{16}H_{17}NO_3$. Anal. calcd for $C_{15}H_{17}NO_2$: C, 70.83; H, 6.32; N, 5.16; O, 17.69 found: C, 70.92; H, 6.28; N, 5.20.

4.5.9 Ethyl(*Z*)-4-((3-oxoquinuclidin-2-ylidene)methyl)benzoate (5b). Yellow solid, mp: 112–115 °C; yield 68%. ^{1}H NMR (400 MHz, $CDCl_3$): δ 1.39–1.42 (3H, t, $-CH_2$); 2.04–2.08 (4H, m, CH_2); 2.65–2.68 (1H, m, CH); 2.99–3.04 (2H, m, CH_2); 3.14–3.23 (2H, m, CH_2); 4.46–4.42 (1H, q, CH_2); 7.04 (1H, s, vinylic proton); 8.02–8.10 (4H, m, ArH). ^{13}C NMR (100 MHz, $CDCl_3$): δ 8.60, 14.3, 25.7, 40.1, 45.6, 47.4, 61.1, 123.8, 129.4, 130.0, 130.7, 131.8, 131.9, 138.1, 146.2, 166.2, 206 Hz. IR (KBr, cm^{-1}): 3387, 3051, 2994, 2963, 2943, 2922, 2871, 1754, 1701, 1679, 1623, 806. ESI/MS 286.2 $[M + 1]^+$ calculated for $C_{17}H_{19}NO_3$. Anal. calcd for: C, 71.56; H, 6.71: N, 4.91; O, 16.82. Found: C, 71.87; H, 6.50; N, 5.13.

4.5.10 Isopropyl(*Z*)-4-((3-oxoquinuclidin-2-ylidene)methyl) benzoate (5c). Yellow solid, mp: 96–97 °C; yield 56%. ^{1}H NMR (400 MHz, $CDCl_3$): δ 1.37–1.39 (6H, d, CH_3); 2.04–2.08 (4H, m, CH_2); 2.66–2.68 (1H, m, CH); 2.99–3.02 (2H, m, CH_2); 3.16–3.21 (2H, m, CH_2); 5.23–5.29 (1H, m, CH_2); 7.04 (1H, s, vinylic proton); 8.02–8.04 (2H, m, ArH). 8.08–8.10 (2H, d, J = 8.4 Hz, ArH). ^{13}C NMR (100 MHz, $CDCl_3$): δ 21.0, 25.7, 40.2, 47.4, 68.5, 123.8, 129.4, 131.8, 138.0, 146.2, 166.2, 206.2. IR (KBr, cm^{-1}): 3057, 2984, 2944, 2964, 2875, 1758, 1724, 1707, 1606, 1458, 810. ESI/MS 300.1 $[M + 1]^+$ calculated for $C_{18}H_{21}NO_3$. Anal. calcd for: C, 72.22; H, 7.07: N, 4.68; O, 16.03. Found: C, 72.45; H, 7.00: N, 4.93.

4.5.11 *sec*-Butyl(*Z*)-4-((3-oxoquinuclidin-2-ylidene)methyl) benzoate (5d). Yellow solid, mp: 100–102 °C; yield 72%. ^{1}H NMR (400 MHz, $CDCl_3$): δ 0.96–1.06 (3H, t, $-CH_3$); 1.34–1.35 (3H, d, $-CH_2$); 1.68–1.74 (2H, m, $-CH_2$); 2.04–2.90 (4H, m, $-CH_2$); 2.67–2.68 (1H, m, CH); 3.00–3.05 (2H, m, CH_2); 3.17–3.23 (2H, m, CH_2); 7.05 (1H, s, vinylic proton); 8.03–8.05 (2H, m, –ArH). 8.08–8.10 (2H, d, J = 8.66 Hz, –ArH). ^{13}C NMR (100 MHz, $CDCl_3$): δ 9.7, 19.5, 25.7, 28.9, 40.1, 47.4, 123.9, 129.4, 131.8, 165.8, 206.2. ESI/MS 313.3 $[M + 1]^+$ calculated for $C_{19}H_{23}NO_2$. Anal. calcd for: C, 72.22; H, 7.07; N, 4.68; O, 16.03. Found: C, 72.45; H, 7.00; N, 4.93.

4.5.12 Cyclopentyl(*Z*)-4-((3-oxoquinuclidin-2-ylidene)methyl) benzoate (5e). Yellow solid, mp: 140–143 °C; yield 43%. ^{1}H NMR (400 MHz, $CDCl_3$): δ 1.47–1.50 (2H, m, $-CH_2$); 1.56–1.64 (2H, m, $-CH_2$); 1.78–1.81 (2H, m, $-CH_2$); 1.92–1.95 (2H, m, $-CH_2$); 2.04–2.08 (4H, m, 2-CH_2); 2.66–2.68 (1H, m, –CH); 2.97–3.04 (2H, m, $-CH_2$); 3.15–3.22 (2H, m, $-CH_2$); 5.02–5.06 (1H, m, –CH); 7.04–7.05 (1H, s, vinylic proton); 8.03–8.13 (4H, m, –ArH). ^{13}C NMR (100 MHz, $CDCl_3$): δ 23.6, 25.4, 25.7, 31.5, 40.1, 47.9, 123.8, 129.4, 130.0, 131.2, 131.7, 131.8, 138.0, 146.2, 165.6, 206.2. IR (KBr, cm^{-1}): 3392, 3056, 2942, 2869, 1755, 1708, 1675, 1624, 805. ESI/MS 325.2 $[M + 1]^+$ calculated for $C_{20}H_{23}NO_3$. Anal. calcd for: C, 73.37; H, 7.70; N, 4.28; O, 14.66. C, 73.08; H, 7.91; N, 4.45.

Acknowledgements

The authors are grateful to the Synth Services Pvt. Ltd, Jarod, Vadodara, India, for financial assistance. The authors thank the DST-PURSE program for Single Crystal X-ray Diffraction, DST FIST program for NMR analysis, Dr Vikram Sarabhai Central instrumentation facility for LCMS and confocal microscopy at the Faculty of Science, The Maharaja Sayajirao University of Baroda and Blue cross pathology lab, Vadodara for haemolytic study.

References

1 Y. Jiao, B.-T. Xin, Y. Zhang, J. Wu, X. Lu, Y. Zheng, W. Tang and X. Zhou, *Eur. J. Med. Chem.*, 2015, **90**, 170.
2 A. Malki, R. Laha and S. C. Bergmeier, *Bioorg. Med. Chem. Lett.*, 2014, **24**, 1184.
3 N. Inceler, A. Yilmaz and S. N. Baytas, *Med. Chem. Res.*, 2013, **22**, 3109.
4 M. I. Rodŕiguez-Franco, I. Dorronsoro, A. Castro, A. Martínez, A. Baďia and J. E. Baños, *Bioorg. Med. Chem.*, 2003, **11**, 2263.
5 J. P. Starck, L. Provins, B. Christophe, M. Gillard, S. Jadot, P. Lo Brutto, L. Quéré, P. Talaga and M. Guyaux, *Bioorg. Med. Chem. Lett.*, 2008, **18**, 2675.
6 L. Farnell, C. R. Ganellin, G. J. Durant, E. Parsons, C. R. Ganellin, J. Port, W. G. Richards, R. Ganellin, C. R. Ganellin, W. Black, H. Pullman, J. Port, M. Kakudo, D. H. Aschman and J. W. Black, *J. Med. Chem.*, 1975, **18**, 666.
7 H. R. Arias, J. J. López, D. Feuerbach, A. Fierro, M. O. Ortells and E. G. Pérez, *Int. J. Biochem. Cell Biol.*, 2013, **45**, 2420.
8 A. Malki, A. B. Pulipaka, S. C. Evans and S. C. Bergmeier, *Bioorg. Med. Chem. Lett.*, 2006, **16**, 1156.
9 A. Malki and E. S. El Ashry, *J. Chemother.*, 2012, **24**, 268.
10 J. Y. Soni, V. Premasagar and S. Thakore, *Lett. Org. Chem.*, 2015, **12**, 277.
11 N. R. Madadi, S. Parkin and P. A. Crooks, *Acta Crystallogr., Sect. E: Struct. Rep. Online*, 2012, **68**, 0730.
12 S. Thakore, M. Valodkar, J. Y. Soni, K. Vyas, R. N. Jadeja, R. V. Devkar and P. S. Rathore, *Bioorg. Chem.*, 2013, **46**, 26.
13 M. Valodkar, R. N. Jadeja, M. C. Thounaojam, R. V. Devkar and S. Thakore, *Mater. Chem. Phys.*, 2011, **128**, 83.

14 K. Vyas, R. N. Jadeja, D. Patel, R. V. Devkar and V. K. Gupta, *Polyhedron*, 2013, **65**, 262.
15 R. Singh, R. N. Jadeja, M. C. Thounaojam, T. Patel, R. V. Devkar and D. Chakraborty, *Inorg. Chem. Commun.*, 2012, **23**, 78.
16 F. Hayat, E. Moseley, A. Salahuddin, R. L. van Zyl and A. Azam, *Eur. J. Med. Chem.*, 2011, **46**, 1897.
17 M. Kutwin, E. Sawosz, S. Jaworski, N. Kurantowicz, B. Strojny and A. Chwalibog, *Nanoscale Res. Lett.*, 2014, **9**, 257.
18 P. J. Shiny, A. Mukherjee and N. Chandrasekaran, *Bioprocess Biosyst. Eng.*, 2014, **37**, 991.
19 M. Nath, M. Vats and P. Roy, *Inorg. Chim. Acta*, 2014, **423**, 70.

Send Orders for Reprints to reprints@benthamscience.ae

Letters in Organic Chemistry, **2015**, *12*, 277-279

An Improved and Simple Route for the Synthesis of 3-Quinuclidinone Hydrochloride

Jigar Y. Soni[a], V. Premasagar[b] and Sonal Thakore[a]*

[a]*Department of Chemistry, Faculty of Science, The M. S. University of Baroda, Vadodara-390002, India.* [b]*Synth Services, Jarod, Vadodara-391520, India*


Sonal Thakore

Received July 11, 2014: Revised December 11, 2014: Accepted January 13, 2015

Abstract: An improved method for the synthesis of 3-quinuclidinone hydrochloride **4** from piperidine-4-carboxylic acid **1** has been described. Reaction of piperidine-4-carboxylic acid **1** with thionyl chloride and ethanol gave ethyl piperidine 4-carboxylate **2**. It was further condensed with methyl chloroacetate in presence of sodium carbonate to give ethyl 1-(2-methoxy-2-oxoethyl)piperidine-4-carboxylate **3**. One pot Dieckmann reaction of **3** in presence of potassium *tert*-butoxide followed by hydrolysis and decarboxylation gave title compound azabicyclo[2.2.2]oct-3-one hydrochloride **4**.

Keywords: 3-quinuclidinone hydrochloride, Dieckmann reaction, isonepecotic acid, Gram scale synthesis.

INTRODUCTION

The quinuclidine is ring system found in a number of natural products [1]. It is also used in preparation of various therapeutically important molecules and also important intermediate and synthesis of some drugs like azasetron, benzoclidine, palonosetron, solifenacin, cevimeline, quinupramine etc [2]. Various quinuclidinone derivatives have been reported to show various biological activities [3-6]. Quinuclidinone derivatives are reported to show anti-cancer [7-8], anti-inflammatory [9], central nervous system stimulating activity [10] and antihistaminic activity [11]. Quinuclidinone has been also used in synthesis of some catalysts which are useful in asymmetric reactions such as aldol reaction [12-14]. Henry and aza Henry reaction [15] and Diels-Alder reaction [16]. Synthesis of quinuclidinone hydrochloride [17] involves multistep organic synthesis. So, we thought of designing relatively simple and safer route for the synthesis of 3-quinuclidinone hydrochloride.

The most useful approach for the construction of quinuclidinone ring is Dieckmann cyclization [18]. Literatures reveal a method for the synthesis of quinuclidinone hydrochloride [17] which has various disadvantages. The main disadvantage is pyridine ring which has serious health concerns. Secondly, it involves a high pressure reaction at a high temperature using very expensive catalyst like Pd/carbon. These disadvantages make this method unsuitable for large scale production. The present method utilizes isonepecotic acid as the starting material so that the hydrogenation step can be avoided. Herewith, we report relatively shorter and safer route which does not involve any harsh conditions, chromatographic purifications or expensive catalyst. Thus this method is cost-effective and easy to scale up.

*Address correspondence to this author at the Department of Chemistry, Faculty of Science, The M. S. University of Baroda, Vadodara-390002, India; Tel: 91-0265-2795552: Fax: 91-0265-2429814;
E-mail: chemistry2797@yahoo.com

RESULT AND DISCUSSION

Esterification of isonipecotic acid **1** in presence of thionyl chloride and ethanol gave ethyl piperidine 4-carboxylate **2** as shown in Scheme **1**. In FTIR, band at 1734 cm^{-1} indicated presence of ester group. In ^1H NMR triplet at δ 1.02 for three protons and quartet at δ 3.88 for two protons indicated presence of ethyl group thus confirming formation of **2**. Further condensation of 2 with mono methyl chloroacetate in presence of base like sodium carbonate gave ethyl 1-(2-methoxy-2-oxoethyl) piperidine-4-carboxylate **3**. In FTIR, band at 1739 cm^{-1} indicated presence of ester group. In ^1H NMR triplet at δ 1.04 and quartet at δ 3.88 for ethyl and singlet at δ 3.51 for methyl thus confirmed formation of **3**. We have tried various reagents and solvents for Dieckmann condensation of ethyl 1-(2-methoxy-2-oxoethyl) piperidine-4-carboxylate **3** to convert it in to ethyl 3-oxoquinuclidine-2-carboxylate as shown in Table **1**. Potassium *tert*-butoxide gave better conversion to ethyl 3-oxoquinuclidine-2-carboxylate compared to sodium methoxide and potassium methoxide but it was very difficult to isolate.

We have also tried to optimize conditions with various acids for hydrolysis and decarboxylation to get azabicyclo[2.2.2]oct-3-one **4** as shown in Table **2**. Optimum result was obtained with HCl while in the case of H_2SO_4 and H_3PO_4 the yield was below 50%. The product was further converted into its hydrochloride salt by purging HCl gas. In FTIR, band at 1748 cm^{-1} indicated presence of carbonyl of which confirmed formation of **4**.

EXPERIMENTAL DETAILS

Reagent grade chemicals and solvents were purchased from commercial supplier and used without purification. TLC was performed on silica gel F254 plates (Merck). Melting points are uncorrected and were measured in open capillary tubes, using a Rolex melting point apparatus. IR spectra were recorded as KBr pellets on Perkin Elmer RX 1 spec-

1875-6255/15 $58.00+.00

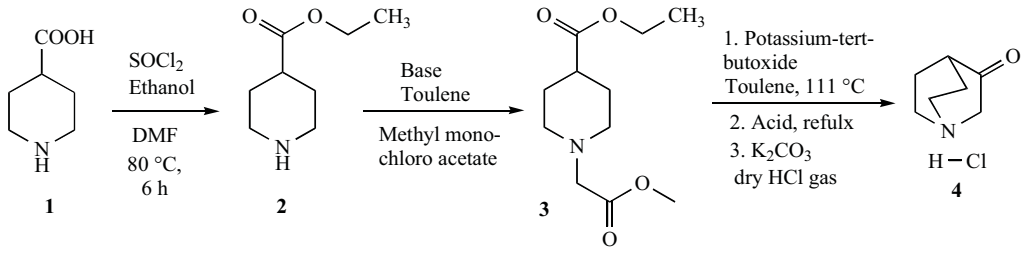

1 **2** **3** **4**

Scheme 1.

Table 1. Reaction condition optimization for the *in situ* cyclisation reaction of quinuclidinone hydrochloride.[a]

Entry	Reagent (mol)	Solvent	Isolated Yield (%)
1	Na\methanol (0.068\0.068)	toluene	No reaction
2	Na\ methanol (0.055\0.055)	xylene	„
3	Na\ methanol (0.072\0.072)	xylene	„
4	28% NaOMe in methanol (0.078)	methanol	„
5	28% NaOMe (0.073)	toluene	„
6	Potassium-*tert*-butoxide (0.163)	toluene	65
7	K\ethanol (0.163\0.163)	toluene	80

[a]Reaction conditions: ethyl1-(2-methoxy-2-oxoethyl) piperidine-4-carboxylate (**3**), concentration: 0.065 mol, reaction time 16 h.

Table 2. Reaction condition optimization for the *in situ* decarboxylation reaction of quinuclidinone hydrochloride.[a]

Entry	Acid	Isolated Yield (%)
1	20% H_2SO_4	22
2	15% H_2SO_4	40
3	20%H_3PO_4	37
4	17% H_3PO_4	39
5	15% H_3PO_4	39
6	10N HCl	60
7	6N HCl	80
8	4N HCl	77

[a]Reaction conditions: ethyl1-(2-methoxy-2-oxoethyl)piperidine-4-carboxylate **3** (0.065 mol), potassium metal (0.16 mol), absolute ethanol (0.17 mol), toluene (200 mL).

trometer. ^{1}H NMR were recorded on Advance Bruker 400 spectrometer (400 MHz) and ^{13}C NMR were recorded on (100 MHz) with $CDCl_3$ or D_2O as solvent and TMS as internal standard.

Ethyl piperidine 4-carboxylate (2) [19]

To a solution of isonipecotic acid **1** (500 g, 3.87 mol) in methanol (1.5 L), thionyl chloride (371 g, 5.03 mol) was added dropwise in nitrogen atmosphere at 0 °C. After addition, reaction was heated to reflux temperature under nitrogen atmosphere for 6 h. Excess methanol was distilled out to give yellow paste which was dissolved in ethyl acetate (1 L) and neutralized with saturated sodium bicarbonate solution. Organic layer was dried by using sodium sulphate and concentrated to afford **2** (560 g, 92%) as colorless liquid. IR (neat) cm^{-1}: 3296, 2949, 2856, 2812, 2739, 1734; ^{1}H NMR ($CDCl_3$, 400 MHz) δ: 1.02-1.05 (3H, t, *J*=7.2 Hz, CH_3), 1.33-1.43 (2H, m, CH_2), 1.63-1.67 (2H, dd, CH_2), 2.14-2.21 (1H, m, CH), 2.37-2.44 (2H, m, CH_2), 2.83-2.87 (2H, m, CH_2), 3.88-3.93 (2H, q, *J*=7 Hz, CH_2). ^{13}C NMR ($CDCl_3$, 100 MHz) δ: 14.1, 29.0, 41.4, 45.6, 60.2, 175.0.

Ethyl 1-(2-methoxy-2-oxoethyl) piperidine-4-carboxylate: (3)

To a solution of ethyl piperidine 4-carboxylate **2** (500 g, 3.18 mol) in dry toluene (1.5 L), sodium carbonate (337 g, 3.18 mol.) was added. Methyl-2-chloroacetate (362 g, 3.3 mol.) was added dropwise at a rate so as to maintain the reaction temperature 45 °C. The reaction mixture was stirred for 4 h at rt. After the completion, the reaction mixture was washed with water till neutral pH. Organic layer was dried and toluene was distilled out under vacuum at 70 °C to afford **3** as yellow liquid (554 g, 76%). IR (neat) cm^{-1}: 2951, 2812, 2775, 1739, 1029. ^{1}H NMR ($CDCl_3$, 400 MHz) δ: 1.04-1.06 (3H, t, *J*=7 Hz, -CH_3), 1.57-1.73 (4H, m, -2CH_2), 2.04-2.10 (3H, m, -CH_2, -CH), 2.69-2.72 (2H, t, -CH_2), 3.03 (2H, s, -NCH_2O), 3.51-3.52 (3H, s, -$0CH_3$), 3.89-3.95 (2H, q, *J*=7 Hz, -CH_2). ^{13}C NMR ($CDCl_3$, 100 MHz) δ 13.9, 27.7, 40.2, 51.3, 52.3, 59.1, 59.9, 170.4, 174.5.

Azabicyclo[2.2.2]oct-3-one hydrochloride: (4) [17]

In dry toluene (1.0 L) potassium-*tert*-butoxide (306.2 g, 2.72 mol) was added under nitrogen atmosphere. Next, the

reaction mixture was refluxed for 30 min under nitrogen atmosphere. Ethyl 1-(2-methoxy-2-oxoethyl)piperidine-4-carboxylate **3** (250 g, 2.18 mol) in 1.0 L dry toluene was added to the reaction mixture dropwise so that addition will complete in 3 h at reflux condition under nitrogen atmosphere. Progress of reaction was monitored by TLC. After completion, the reaction mixture was cooled to 0-5 °C and cold 6 N HCl (1.3 L) was added. The aqueous layer was separated and refluxed for 14 h for hydrolysis and successive decarboxylation. Reaction mass was neutralized by adding saturated K_2CO_3 solution and product was extracted in ethyl acetate (1.5 L). Organic layer was acidify by purging dry HCl gas and was evaporated to afford **4** as colorless solid (140 g, 80%).

Mp 300 °C. [17], IR: (neat) cm^{-1}: 2965, 2907, 2764, 1748; ^1H NMR (D_2O, 400 MHz): δ 1.79-1.81 (0.5H, m), 2.00-2.10 (1.5H, m), 2.17-2.24 (1H, m), 2.69-2.70 (0.5H, t), 3.10-3.18 (1H, m), 3.29-3.36 (1H, m), 3.41-3.49 (1H, m), 3.91 (1H, s). ^{13}C NMR (D_2O, 100 MHz): δ 25.5, 25.7, 40.0, 47.3, 47.4, 102.3, 118.8, 122.6, 123.6, 127.4, 132.0, 132.12, 132.3, 133.5, 137.4, 138.3, 146.1, 147.1, 168.7, 205.8.

CONCLUSION

An efficient three step method for the synthesis of 3-quinuclidinone hydrochloride has been developed. The present method utilizes isonepecotic acid as the starting material which omits hydrogenation step and use of expensive catalyst. This method has advantage of being cost effective, facile and safe for the synthesis of 3-quinuclidinone hydrochloride.

CONFLICT OF INTEREST

The authors confirm that this article content has no conflict of interest.

ACKNOWLEDGEMENTS

One of the authors JYS would like to thank Dr. Chirag Patel and Mr. Hemal Soni Oxygen healthcare Ltd, Ahmadabad for fruitful discussion.

SUPPLEMENTARY MATERIALS

Supplementary material is available on the publisher's web site along with the published article.

REFERENCES

[1] (a) Kaufman, T. S.; Rúveda, E. a The Quest for Quinine: Those who won the battles and those who won the war. *Angew. Chem. Int. Ed.* **2005**, *44*, 854–85. (b) Turner, R. B.; Woodward, R. B. Chapter 16 The Chemistry of the Cinchona Alkaloids. In the alkloids: Chemistry amd physiology, Academic Press, 1953; Volume 3, pp. 1-63. (c) Uskoković, M. R.; Grethe, G. Chapter 5 The Cinchona Alkaloids. In the Alkloids: Chemistry and Physiology, Ed.; Academic Press, 1973; Vol. 14, pp. 181-223.

[2] Mazurov, A.; Klucik, J.; Miao, L.; Phillips, T. Y.; Seamans, A.; Schmitt, J. D.; Hauser, T. A.; Johnson, R. T.; Miller, C. 2-(Arylmethyl)-3-substituted quinuclidines as selective α-7 nicotinic receptor ligands. *Bioorg. Med. Chem. Lett.* **2005**, *15*, 2073–2077.

[3] Yang, D.; Soulier, J. L.; Sicsic, S.; Mathé-Allainmat, M.; Brémont, B.; Croci, T.; Cardamone, R.; Aureggi, G.; Langlois, M. New Esters of 4-Amino-5-chloro-2-methoxybenzoic acid as Potent Agonists and Antagonists for 5-HT_4 Receptors. *J. Med. Chem.* **1997**, *40*, 608–621.

[4] Bos, M.; Canesso, R. EPC-Synthesis of (S)-3-Hydroxy-3-mercaptomethylquinuclidine, a Chiral Building Block for the Synthesis of the Muscarinic Agonist AF 102B. *Heterocycles*, **1994**, *38*, 1889-96.

[5] Trost, B. M. On Inventing Reactions for Atom Economy. *Acc. Chem. Res.* **2002**, *35*, 695–705.

[6] Frackenpohl, J.; Hoffmann, H. M. R. Synthesis of Enantiopure 3-Quinuclidinone Analogues with Three Stereogenic Centers: (1*S*,2*R*,4*S*) – and (1*S*,2*S*,4*S*)-2-(Hydroxymethyl)-1-azabicyclo[2.2.2] octane-5-one and Stereocontrol of Nucleophilic Addition to the Carbonyl Group. **2000**, *65* 3982-3996.

[7] Bykov, V. J. N.; Issaeva, N.; Selivanova, G.; Wiman, K. G. Mutant p53-dependent growth suppression distinguishes PRIMA-1 from known anticancer drugs: a statistical analysis of information in the National Cancer Institute database. *Carcinogenesis*, **2002**, *23*, 2011-2018.

[8] Bykov, V. J. N.; Issaeva, N.; Shilov, A.; Hultcrantz, M.; Pugacheva, E.; Chumakov, P.; Bergman, J.; Wiman, K. G,; Selivanova, G. Restoration of the tumor suppressor function to mutant p53 by a low-molecular-weight compound. *Nat. Med.* **2002**, *8*, 282-288.

[9] Warawa, E. J.; Mueller, N. J.; Jules, R. Quinuclidine chemistry. 2.[1] Synthesis and Antiinflammatory properties of 2-Substituted Benzhydryl-3-quinuclidinols. *J. Med. Chem.,* **1974**, *17*, 497-501.

[10] Warawa, E. J.; Mueller, N. J.; Gylys, J. A. Quinuclidine chemistry. 3.[1] β-*cis*-2-(4'-Chlorobenzhydryl)-3-quinuclidinol, a new central nervous system stimulant. Importance of the benzhydryl configuration. *J. Med. Chem.,* **1975**, *18*, 71-74.

[11] Gonnot, V.; Nicolas, M.; Mioskowski, C.; Baati, R. Expedient synthesis of mequitazine an antihistaminic drug by palladium catalyzed allylic alkylation of sodium phenothiazinate. *Chem. Pharm. Bull.* **2009**, *57*, 1300-1302.

[12] Yoon, T. P.; Jacobsen, E. N. Privileged Chiral Catalysts. *Science,* **2003**, *299*, 1691-3.

[13] Ma, B.; Parkinson, J. L.; Castle, S. L. Novel *Cinchona* alkaloid derived ammonium salts as catalysts for the asymmetric synthesis of β-hydroxy α-amino acids via aldol reactions. *Tetrahedron Lett.* **2007**, *48*, 2083-2086.

[14] Jew, S.; Yoo, M.; Jeong, B.; Park, I. Y.; Park, H. An unusual electronic effect of an aromatic-F in phase-transfer catalysts derived from *Cinchona* -alkaloid. *Org. Lett.,* **2002**, 5-8.

[15] Marcelli, T.; Haas, R. N. S. V.; Maarseveen, J. H. V.; Hiemstra, H. Asymmetric organocatalytic henry reaction. *Angew. Chem. Int. Ed.* **2006**, *45*, 929–31.

[16] Riant, O.; Kagan, H. B. Asymmetric diels-alder reaction catalyzed by chiral bases. *Tetrahedron Lett.* **1989**, *30*, 7403–7406.

[17] Daeniker, H. U.; Grob, C. A. 3-Quinuclidone hydrochloride. *Org. Synth. Coll. Vol.,* **1964**, *44*, 86-90.

[18] Snow, R. J.; Baker, R.; Herbert, R. H.; Hunt, I. J.; Merchant, K. J.; Saunders, J. The synthesis of 5- and 6-substituted quinuclidine-3-carboxylic esters: Intermediates for novel muscarinic ligands. *J. Chem. Soc. Perkin Trans. 1* **1991**, 409-420.

[19] (a) Nguyen, W.; Howard, B. L.; Jenkins, D. P.; Wulff, H.; Thompson, P. E.; Manallack, D. T. Structure-activity relationship exploration of Kv1.3 blockers based on diphenoxylate. *Bioorg. Med. Chem. Lett.,* **2012**, *22*, 7106-9. (b) Tripathi, R. C.; Pandey, S. K.; Kar, K.; Dikshit, M.; Saxena, A. K. Synthesis and SAR studies of 1-substituted-n-(4- alkoxycarbonylpiperidin-1-yl)alkanes as potent antiarrhythmic agents. *Bioorg. Med. Chem. Lett.,* **1999**, *9*, 2693–2698. (c) Diouf, O.; Depreux, P.; Chavatte, P.; Poupaert, J. H. Synthesis and preliminary pharmacological results on new naphthalene derivatives as 5-HT_4 receptor ligands. *Eur. J. Med. Chem.,* **2000**, *35*, 699-706.

Bioorganic Chemistry 46 (2013) 26–30

Contents lists available at SciVerse ScienceDirect

Bioorganic Chemistry

journal homepage: www.elsevier.com/locate/bioorg

Synthesis and cytotoxicity evaluation of novel acylated starch nanoparticles

Sonal Thakore [a,*], Mayur Valodkar [a], Jigar Y. Soni [a], Komal Vyas [a], Rajendrasinh N. Jadeja [a], Ranjitsinh V. Devkar [b], Puran Singh Rathore [a]

[a] Department of Chemistry, Faculty of Science, The Maharaja Sayajirao University of Baroda, Vadodara 390 002, Gujarat, India
[b] Department of Zoology, Faculty of Science, The Maharaja Sayajirao University of Baroda, Vadodara 390 002, Gujarat, India

ARTICLE INFO

Article history:
Received 7 June 2012
Available online 13 October 2012

Keywords:
Acylated starch nanoparticles
Cytotoxicity
DNA binding

ABSTRACT

Starch nanoparticles (StNPs) were acylated under ambient conditions to obtain various nanosized derivatives formed stable suspension in water and soluble in organic solvents. The degree of substitution (DS) was determined using ^{1}H NMR technique. The cytotoxicity potential of the derivatised StNPs was evaluated in mouse embryonic fibroblast (3T3L1) cells and A549 tumor cell line using MTT cell viability assay. Other parameters that determine the oxidative stress viz., reactive oxygen species (ROS) generation, intracellular reduced glutathione (GSH), superoxide generation and acridine orange/ethidium bromide staining were also investigated. The present study led to the conclusion that cytotoxic activity of acylated starch nanoparticles was dependent on their dosage, DS and type of substitution. The non-toxic nature in non-cancerous cells reveals that the nanoparticles (NPs) can be used for cancer therapy and drug delivery. The nanoparticles also offered reasonable binding propensity with CT-DNA.

1. Introduction

Cytotoxic drugs continue to play a major role in cancer therapy but often produce side effects, especially through the destruction of lymphoid and bone marrow cells [1]. Therefore, strategic improvements in cancer therapy are needed to improve efficacy while decreasing side effects. Over the past decades, nanoparticles (NPs) have been of great interest in applications for biological fields such as drug delivery systems [2,3] and anticancer applications [4]. The antitumor activities of natural biopolymer chitosan and its NPs are well reported [5]. Another abundant polysaccharide starch, is relatively, more competent than chitosan due to its low cost, easy availability and better solubility but suffers from drawback of hydrophilic nature. The synthesis of starch nanoparticles (StNPs) reported by Dufresne et al. [6] paved the way for the development of novel nanosized starch derivatives which can offer great potential for use in diverse medicinal applications. The evaluation of the *in vitro* cytotoxicity of a biomaterial is the initial step of biocompatibility study. Hence we investigated the cytotoxic potential of hydrophobic, nanosized, starch derivatives for two different applications viz. potential anticancer agents and promising biocompatible drug carriers. In the past our group has extensively studied the cytotoxicity evaluation of metal nanoparticles [4,7] as well as starch metal nanoconjugates [8] with prokaryotic as well as eukaryotic cells. In this paper we have reported the interesting interaction of nanosized acyl derivatives of starch with A549 human lung carcinoma cells as well as mouse embryonic fibroblast (3T3L1) cells and CT-DNA.

2. Experimental

Starch nanocrystals (StNPs) were prepared according to the procedure described elsewhere [6]. Acylation of StNPs was carried out by dispersion in aqueous alkali followed by room temperature reaction with various acid chloride or anhydride [9]. Attempts were made to carry out the synthesis under ambient conditions so as to preserve the nanosize. Four type of derivatives were synthesized viz. St-palmiate, St-benzoate, St-phthalate and St-cinnamate. The product was collected by centrifugation and purified (Supporting information).

3. Results and discussion

The acylation was confirmed by spectroscopic analysis. The characteristic peaks in the FT-IR spectra (Supporting information) of all the starch nanoparticles are the stretching and bending vibrations of hydrogen bonded –OH groups observed at 3400 and 1650 cm^{-1}. The FT-IR spectra after acylation, showed a carbonyl absorption band at 1736, 1740, 1742 and 1750 cm^{-1} for palmiate, benzoate, cinnamate and phthalate starch nanoparticles respectively. In case of aromatic derivatives the peaks due to stretching and bending of aromatic –C–H appear around 3000 and 800 cm^{-1} respectively.

The ^{1}H NMR data of the starch nanoparticles is given below.

* Corresponding author. Fax: +91 0265 2581102.
E-mail address: chemistry2797@yahoo.com (S. Thakore).

0045-2068/$ - see front matter © 2012 Elsevier Inc. All rights reserved.
http://dx.doi.org/10.1016/j.bioorg.2012.10.001

StNPs: 5.1 (w, 1H, H-1), 3.31 (s, 1H, H-2), 3.96 (w, 1H, H-3), 3.37 (s, 1H, H-4), 3.08 (w, 1H, H-4 end group), 3.60 (s, 1H, H-5), 3.65 (s, 2H, H-6,60), 5.42 (m, 1H, H-2), 5.44 (m, 1H, H-3) [2].
St-phthalate NPs (DS = 2.63): ^{1}H NMR (400 MHz, $CDCl_3$) δ 11.0 (s, 1H), 7.89 (d, J = 6.8, 2H), 7.81 (d, J = 6.3, 2H), 4.95 (s, J = 2, 1H), 4.01 (s, J = 2.2, 1H), 3.57 (s, J = 2.1, 1H), 3.23 (s, J = 2.2, 1H).
St-cinnamate NPs (DS = 2.59): ^{1}H NMR (400 MHz, $CDCl_3$) δ 7.91 (d, J = 6.4, 2H), 7.67 (d, J = 6.3, 2H), 6.45 (d, J = 2.2, 2H), 4.97 (s, J = 2.1, 1H), 4.45 (s, J = 2.3, 1H), 4.11 (s, J = 2.1, 1H), 3.44 (s, J = 2.2, 1H).
St-benzoate NPs (DS = 1.98): ^{1}H NMR (400 MHz, $CDCl_3$) δ 8.12 (s, J = 6.5, 2H), 7.52 (s, J = 6.3, 2H), 5.5 (s, J = 2.3, 1H), 5.01 (s, J = 2.4, 1H), 4.45 (d, J = 2.5, 1H), 3.52 (s, J = 2.1, 1H).
St-palmiate NPs (DS = 2.49): ^{1}H NMR (400 MHz, $CDCl_3$) δ 4.98 (s, J = 2.2, 1H), 4.04 (s, J = 2.1, 1H), 3.47 (s, J = 2.3, 1H), 2.97 (s, J = 2.4, 1H), 2.34 (s, J = 2.1, 2H), 1.67 (s, J = 2.4, 2H), 1.21 (s, J = 2.3, 2H), 0.85 (t, J = 2.4, 3H).

Transmission electron micrographs (TEMs) (Fig. 1) showed that after acylation the size of the StNPs decreases. The platelet-like particles of the unmodified StNPs [6] (Supporting information) became somewhat spherical after modification with the diameter ranged from 40 to 50 nm, due to blocking of hydroxyl groups which leads to individualization of NPs [10]. The results of DLS (Supporting information) also showed a single narrow distribution with average particle size in the range of 30–50 nm. The results of thermal analysis (Supporting information) reveal that gelatinization temperature was lower while thermal stability was higher for acylated StNPs [3]. This suggests improved processibility which is necessary for drug delivery applications.

The *in vitro* cytotoxicity was evaluated at various doses by exposure of A549 cells as well as 3T3L1 cells to acylated StNPs. Upto 1000 μg/mL concentration the cell viability was recorded to be higher than 85% even after 72 h (data not shown). This biocompatibility was suggestive of the potential of these materials for use as nanocarriers of drug molecules. A dose range of 1000–10,000 μg/mL recorded moderate cytotoxicity in 3T3L1 cells (Supporting information) while StNPs induced practically no cell death. At this dose, in tumor cells interesting dose dependent cytotoxicity was observed within 24 h (Fig. 2a). Among all the NPs tested herein, St-cinnamate NPs showed highest cytotoxicity (Table 1 Supporting information) and its highest dose (10,000 μg/mL) recorded nearly 80% cytotoxicity (Fig. 2a). On the other hand, St-palmitate NPs recorded lowest cytotoxic potential, probably because of its completely aliphatic structure. Cytotoxicity differences between the acylated starch derivatives are probably due to the different hydrophobicity and charge density of StNPs. In addition, other parameters such as the degree of substitution and type of substitution also determine the extent of cytotoxic activity of StNPs. There may be a structure activity relationship which requires further investigation.

In biological activities, cell must interact with the extracellular environment which is generally through chemical, electrical or mechanical signaling. In the present studies, DS of acylated starch NPs are $\geqslant$2 which indicates the hydrophobic nature of acylated starch NPs. Cytotoxicity is reported to increase with increasing hydrophobicity [11]. Based on this it can be concluded that there is hydrophobic interaction between tumor cells and starch derivatives which is responsible for cytotoxicity.

Molecules at nanoscale may be able to help overcome the undesirable effects of traditional chemotherapeutic agents by maximiz-

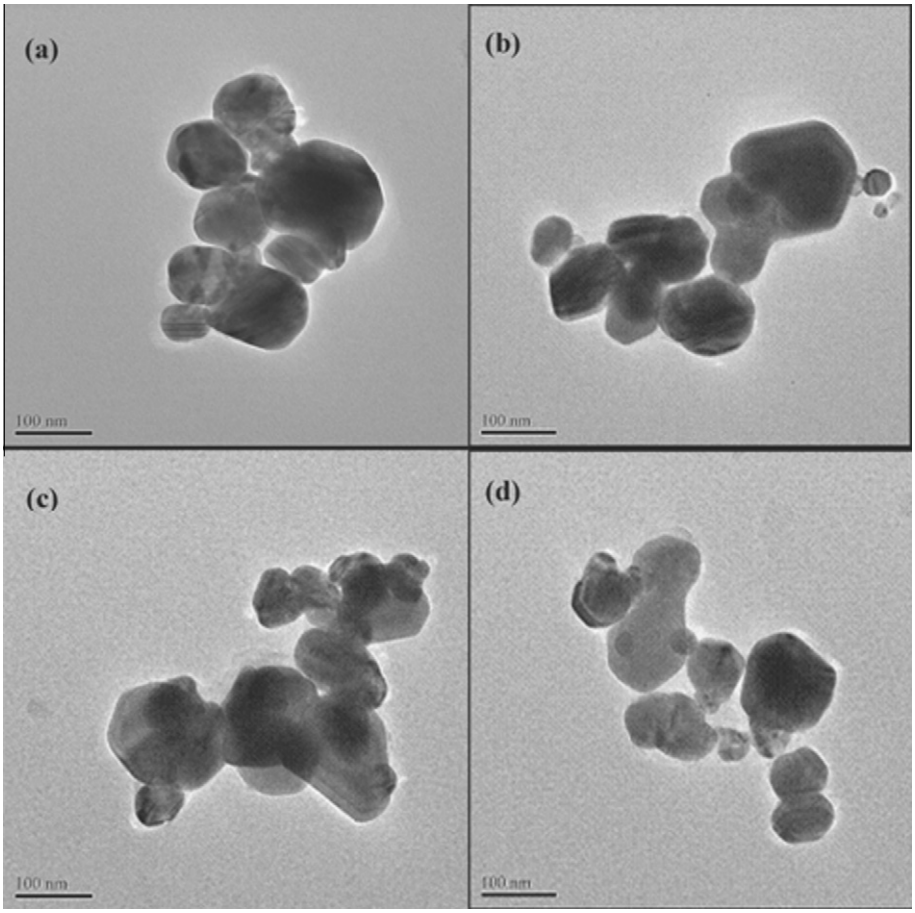

Fig. 1. TEM images of (a) St-phthalate, (b) St-cinnamate, (c) St-benzoate and (d) St-palmiate nanoparticles.

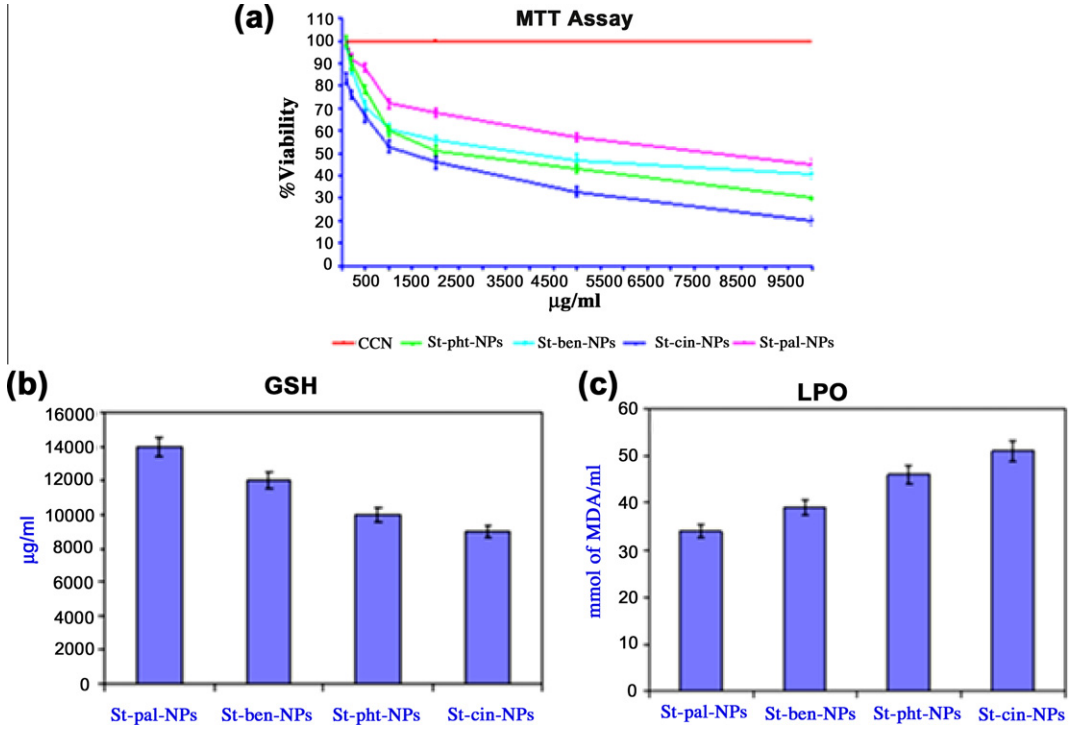

Fig. 2. Effect of modified starch nanoparticles exposure on cell viability (a) MTT assay, (b) reduced glutathione content and (c) lipid peroxidation in A549 cells. Results are expressed as mean ± SEM for $n = 3$ (replicates). Where NS = non-significant, $^{*}p < 0.05$, $^{**}p < 0.01$ and $^{***}p < 0.001$ compared to untreated cells.

ing their availability at the target tumor site and minimizing noxious effects on healthy tissue [12]. Tumor cells overexpress many receptors and biomarkers, which can be used as targets to deliver cytotoxic agents into tumors [13]. Cancer cells are highly metabolic and porous in nature and are known to internalize solutes rapidly compared to normal cells. Therefore, we hypothesized that acyl StNPs will also show preferential internalization within cancer cells. Tumor sites possess unique vasculature characteristics that can be easily exploited by nanoscale systems to efficiently reach cancer targets. The endothelial cells in tumor vasculature have loose interconnections and focal intercellular openings. These breaks in the endothelial cell lining range in size between 100 and 1000 nm, and nanoparticles (NPs) can easily extravasate these openings. This phenomenon of localizing NPs in the leaky vasculature of tumor tissues is an example of passive targeting [12].

The cytotoxicity of chitosan NPs and derivatives has been attributed to positive surface charge [5]. However zeta potential measurements of acylated StNPs (Table 1 Supporting information) showed that they have negative surface charge. This is because, neither size nor zeta potential alone determine the optimal cellular response induced by NPs [14]. It has also been proposed that, in regions where the columbic repulsion of similar charges is not too pronounced, the presence of a high electric field may cause local electroporation. So, high electrical fields of the NPs of about 50 nm, which may succeed even with negative zeta potential, may eventually lead to cytotoxicity. This phenomenon is known to facilitate permeation of various nanoscale objects through biological membranes. It is reported in literature, that the proteins from the growth media adsorb to the surfaces of both cationic and anionic NPs, increase their hydrodynamic radius, and flips their charge immediately to similar negative value of the serum proteins in the original media [15]. Thus size, aggregation state, surface charge and surface chemistry would be significantly modified via electrostatic screening which in turn could influence their ability to interact with or enter cells [16,17]. Therefore, NPs that had a positive effective surface charge upon preparation are no longer cationic in the cellular media. This is important when considering the molecular effect of charge on toxicity and cellular uptake, and argues against the simple picture, still propagated in the literature, that cationic nanoparticles disrupt the negatively charged cellular membrane by electrostatic interactions. Protein adsorption to the NPs surface can mediate the uptake of the nanomaterial via receptor mediated endocytosis [18,19]. This is believed to be the reason for the interaction of the nanosized derivatives with biological systems.

Oxidative stress is often considered as the main cause for stimulation of cytotoxicity that is induced by natural or synthetic toxic agents [20]. Toxicity of NPs is exerted in form of transferring electron from molecular oxygen or by blockade of electron transport chain through an unknown mechanism [21,22]. Cellular response to increased oxidative stress results in a compromised status of endogenous antioxidants such as reduced glutathione (GSH). Also, free radical induced membrane damage caused due to lipid peroxidation (LPO) results in leakage of cellular enzymes [23]. Hence, biochemical estimation of GSH and LPO are reliable markers of cell damage caused due to production of free radicals. GSH is considered to be the first line of cellular defense for cells under various conditions of oxidative stress [24]. GSH is used as a co-substrate by enzymes; GPX and GR for reduction of hydrogen peroxide and lipid peroxides [24]. It is evident from Fig. 2b that 10,000 µg/mL of acylated starch NPs dose shows significantly low content of cellular GSH. This indicates that at high concentration of 10,000 µg/mL these NPs show cytotoxic nature (Fig. 2b).

Damage of cellular membrane due to LPO is the major cause of cell death and hence, its integrity is pivotal for its survival. In the present study, a 10,000 µg/mL dose of acylated starch NPs recorded higher LPO indices (Fig. 2c). Significantly elevated indices of LPO and lower activity of GSH showed that acylated starch NPs were cytotoxic in nature.

AO/EB staining for cell viability depicted a cell death with maximum number of EB positive cells (red[1] colored) recorded in high-

[1] For interpretation of color in Fig. 3, the reader is referred to the web version of this article.

est dose (10,000 μg/mL) of acylated starch NPs (Fig. 3). Previous studies have reported polysaccharide NP induced cytotoxicity against various tumor cell resulting due to oxidative damage to the cell membrane and mitochondrial dysfunction [22,25]. Similar alterations observed in our study are in accordance with these reports and thus establish the doses and the resultant cellular damage caused by acylated StNPs.

The binding interaction of many organic carcinogens such as polycyclic aromatic hydrocarbons with DNA is the key step in their genotoxic effect. Titration with UV absorption spectroscopy is an effective method to examine the binding mode of DNA with the molecules [26]. In general, the spectra of the compounds show UV absorption bands that are usually symmetrical with no obvious splitting. In the UV region, compounds exhibited bands between 240 and 320 nm, which are assigned to the $\pi \rightarrow \pi^*$ transitions, due to long living triplet excited state. Hypochromism results from the contraction of DNA helix axes as well as the conformational changes on molecule of DNA, while hyperchromism results from the secondary damage of DNA double helix structure [27,28]. Upon increasing concentration of CT DNA, the UV region exhibited an increase in absorption intensity 'hyperchromic' effect with a blue shift of 2–10 nm in $\pi \rightarrow \pi^*$ region (Fig. 4a and Supporting information). The strong hyperchromic effect with a blue shift is suggestive of higher binding propensity to CT DNA due to stabilization of the nanoparticle–DNA adduct. These changes are typical of compounds bound to double stranded DNA through non-covalent interaction [29]. In the present case, the complete intercalation of the compounds between a set of adjacent base pairs seems sterically impossible, but some partial intercalation can be envisioned [30].

Enhancement of the fluorescence emission when binding with the biomacromolecules (such as DNA and proteins), is a very useful fluorescent probe in genomics and proteomics [31]. In present study we found that luminescence was not observed for compounds either in DMSO or in presence of DNA. Hence, competitive binding studies using ethidium bromide (EB) bound DNA was carried out. EB is a conjugate planar molecule. Its fluorescence intensity is very weak but it is greatly enhanced when EB is specifically intercalated into the adjacent base pairs of double stranded DNA. The enhanced fluorescence can be quenched by the addition of a second molecule [32]. The addition of compounds to DNA-EB sys-

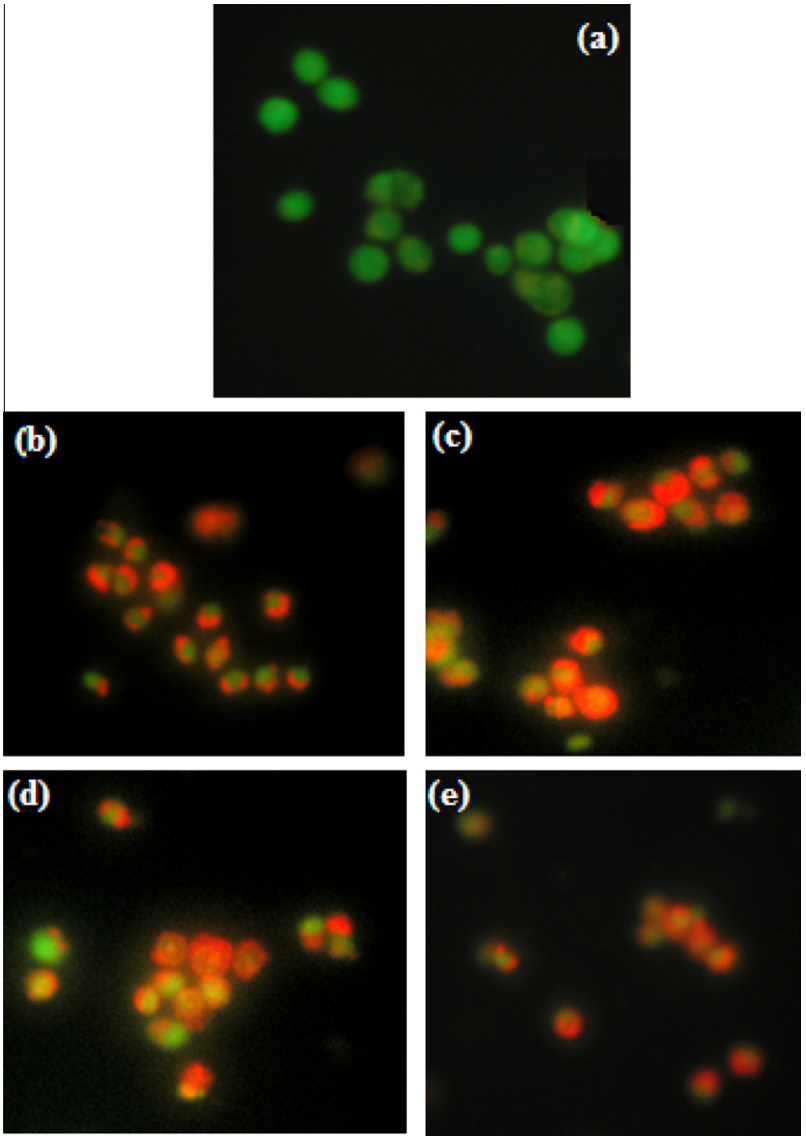

Fig. 3. AO/EB photomicrographs of stained A549 cells exposed to (a) 0 mg/mL and 10 mg/mL concentration of (b) St-palmiate, (c) St-benzoate, (d) St-phthalate and (e) St-cinnamate nanoparticles. Results are expressed as mean ± SEM for $n = 3$ (replicates). Where NS = non-significant, $^{*}p < 0.05$, $^{**}p < 0.01$ and $^{***}p < 0.001$ compared to untreated cells.

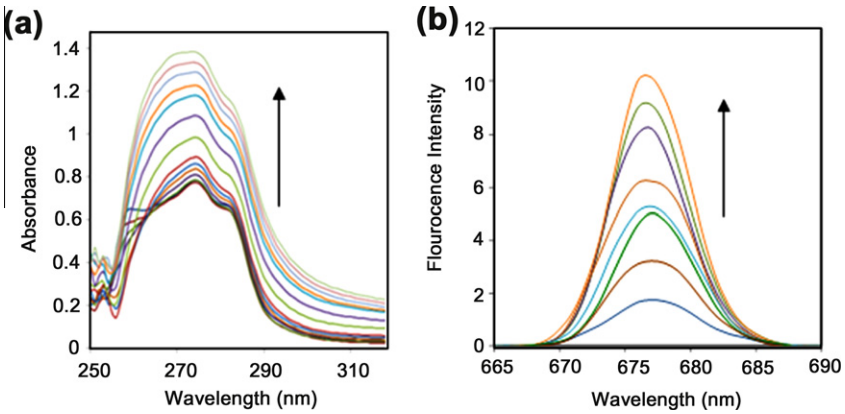

Fig. 4. (a) Absorption spectra of the St-benzoate NPs (0.1 mg/mL) without and with CT-DNA at different concentrations (0.05, 0.10, 0.15, 0.20, 0.25, 0.30, 0.35, 0.40, 0.45, 0.50, 0.55 and 0.60 mL of stock solution). The arrow shows the intensity changes on increasing the acylated StNPs concentration, (b) emission spectra of EB bound to DNA in the absence and presence of the St-benzoate NPs. [EB] = 40 μM, [DNA] = 50 mL, [St-benzoate NPs] = 2, 4, 6, 8, 10, 12 and 14 μL, respectively; λ_{mex} = 340 nm. The arrow shows the intensity changes on increasing the acylated StNPs concentration.

tem displayed an increase in emission intensity of the DNA-EB system (Fig. 4b and Supporting information). Increase in fluorescent intensity indicates that the acylated StNPs has not completely intercalated into the DNA helix, as complete intercalation would decrease the emission intensity due to the replacement of the intercalated EB from DNA. The observed results suggest that the nanoparticles can make a contraction in the helix axis of DNA [31,33]. The binding affinity seems to follow the order St-Pal-NPs ⩾ St-Pht-NPs > St-Cin-NPs > St-Ben-NPs. Aliphatic derivative has greater binding probably due to more flexible structure. The presence of additional carboxyl group as in phthalate or extension of conjugation as in cinnamate both increase the binding affinity.

4. Conclusions

The present study reports for the first time, cytotoxic potential of the acylated starch nanoparticles along with its biocompatible nature and warrants further evaluation at preclinical and clinical levels. The noncytotoxicity to non-cancerous cells and useful thermal properties suggest promising drug delivery applications of these materials at lower concentrations while higher doses would be useful as anticancer agents. The cytotoxicity of derivatives with aromatic groups and high degree of substitution was higher relative to those containing aliphatic group. The details of the mechanism of action, especially to clarify the mode of interaction with tumor cells, effect of degree of substitution and particle size are now under investigation. Despite negative zeta potential the nanoparticles exhibited reasonable biding propensity with CT-DNA, although complete intercalation was not observed.

Acknowledgments

The authors are grateful to Sophisticated Analytical Instrument Facility (SAIF), Shilong for carrying out TEM analysis. Special thanks to Dr. Menaka C. Thounaojam and Dr. Ravirajsinh N. Jadeja, Department of Zoology, for cytotoxicity studies.

Appendix A. Supplementary material

Supplementary data associated with this article can be found, in the online version, at http://dx.doi.org/10.1016/j.bioorg.2012.10.001.

References

[1] J.K. Lee, H.S. Lim, J.H. Kim, Med. Chem. Lett. 12 (2002) 2949–2951.
[2] M.J. Santander-Ortegab, T. Stauner, B. Loretz, J.L. Ortega-Vinuesa, D. Bastos-González, G. Wenz, U.F. Schaefer, C.M. Lehr, J. Controlled Release 85 (2010) 85–92.
[3] C.K. Simi, A. Emilia Abraham, Bioprocess Biosyst. Eng. 30 (2007) 173–180.
[4] M. Valodkar, R.N. Jadeja, M.C. Thounaojam, R.V. Devkar, S. Thakore, Mater. Chem. Phys. 128 (2011) 83–89.
[5] L. Qi, Z. Xu, X. Jiang, Y. Li, M. Wang, Bioorg. Med. Chem. Lett. 15 (2005) 1397–1399.
[6] J.L. Putaux, S. Molina-Boisseau, T. Momaur, A. Dufresne, Biomacromolecules 4 (2003) 1198–1202.
[7] M.C. Thounaojam, R.N. Jadeja, M. Valodkar, P.S. Nagar, R.V. Devkar, S. Thakore, Food Chem. Toxicol. 49 (2011) 2990–2996.
[8] M. Valodkar, P.S. Rathore, R.N. Jadeja, M.C. Thounaojam, R.V. Devkar, S. Thakore, J. Hazard. Mater. 201–202 (2012) 244–249.
[9] H. Namazi, A. Dadkhah, Carbohydr. Polym. 79 (2010) 731–737.
[10] M. Valodkar, S. Thakore, Carbohydr. Res. 345 (2010) 2354–2360.
[11] J.Y. Je, Y.S. Cho, S.K. Kim, Bioorg. Med. Chem. Lett. 16 (2006) 2122–2126.
[12] T. Lei, S. Srinivasan, Y. Tang, R. Manchanda, A. Nagesetti, A. Fernandez-Fernandez, et al., Nanomed. Nanotechnol. 7 (2011) 324–332.
[13] P. Kesharwani, R.K. Tekade, V. Gajbhiye, K. Jain, N.K. Jain, Nanomed. Nanotechnol. 7 (2011) 295–304.
[14] H.K. Patra, A. Dasgupta, Nanomed. Nanotechnol. 8 (2011) 115–121.
[15] A.M. Alkilany, P.K. Nagaria, C.R. Hexel, T.J. Shaw, C.J. Murphy, M.D. Wyatt, Small 5 (2009) 701–708.
[16] T. Cedervall, I. Lynch, M. Foy, Angew. Chem. Int. Ed. 46 (2007) 5754–5756.
[17] A.M. Alkilany, C.J. Murphy, J. Nanopart. Res. 12 (2010) 2313–2333.
[18] S.D. Conner, S.L. Schmid, Nature 422 (2003) 37–44.
[19] L.C. Henderson, J.M. Altimari, G. Dyson, L. Servinis, B. Niranjan, G.P. Risbridger, Bioorg. Chem. 40 (2012) 1–5.
[20] J. Boonstra, J.A. Post, Gene 337 (2004) 1–13.
[21] J.F. Turrens, J. Physiol. 552 (2003) 335–344.
[22] P.V. AshaRani, G.L.K. Mun, M.P. Hande, S. Valiyaveettil, ACS Nano 3 (2009) 279–290.
[23] M.C. Thounaojam, R.N. Jadeja, D.S. Dandekar, R.V. Devkar, A.V. Ramachandran, Exp. Toxicol. Pathol. 63 (2011) 351–357.
[24] M. Valodkar, R.N. Jadeja, M.C. Thounaojam, R.V. Devkar, S. Thakore, Mater. Sci. Eng. 31 (2011) 1723–1728.
[25] S.M. Hussain, K.L. Hess, J.M. Gearhart, K.T. Geiss, J. Schlager, J. Toxicol. In Vitro 19 (2005) 975–983.
[26] T.M. Kelly, A.B. Tossi, D.J. McConnell, T.C. Strekas, Nucleic Acids Res. 13 (1985) 6017–6034.
[27] J.K. Barton, A.T. Danishefsky, J.M. Goldberg, J. Am. Chem. Soc. 106 (1984) 2172–2176.
[28] C.S. Chow, J.K. Barton, Methods Enzymol. 212 (1992) 219–242.
[29] T. Hirohama, Y. Kuranuki, E. Ebina, T. Sugizaki, H. Arii, M. Chikira, P.T. Selvi, M. Palaniandavar, J. Inorg. Biochem. 99 (2005) 1205–1219.
[30] R.S. Kumar, S. Arunachalam, V.S. Periasamy, C.P. Preethy, A. Riyasdeen, M.A. Akbarsha, Polyhedron 27 (2008) 1111–1120.
[31] J. Kang, H. Wu, X. Lu, Y. Wang, L. Zhou, Spectrochim. Acta A 61 (2005) 2041–2047.
[32] J.B. Lepecq, C. Paoletti, J. Mol. Biol. 27 (1967) 87–106.
[33] Z.C. Yong, X.X. Li, Y. Pin, Biochemistry (Moscow) 72 (2007) 27–37.